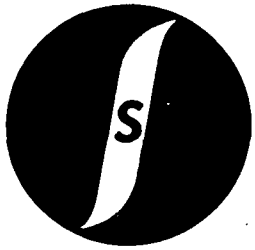

COMMUNICATION PERFORMANCE OVER THE TDRS MULTIPATH/INTERFERENCE CHANNEL

Dr. J. Jenny
D. Gaushell
Dr. P. Shaft

19 August 1971

ESL, INCORPORATED

ELECTROMAGNETIC SYSTEMS LABORATORIES
495 JAVA DRIVE • SUNNYVALE • CALIFORNIA

ESL-TM239
Copy No. 11

ESL INCORPORATED

Electromagnetic Systems Laboratories

Sunnyvale, California

Technical Memorandum
No. ESL-TM239
19 August 1971

COMMUNICATION PERFORMANCE OVER THE TDRS MULTIPATH/INTERFERENCE CHANNEL

Dr. J. Jenny
D. Gaushell
Dr. P. Shaft

APPROVED FOR PUBLICATION. . . . . Lewis R. Franklin

Lewis R. Franklin
Manager
Signal Systems Laboratory

Prepared Under Contract No. NAS5-20228

This Document Consists of 98 Pages

Copy No. 11 of 40 Copies

CONTENTS

Section		Page
1.	INTRODUCTION AND SUMMARY OF RESULTS	1-1
1.1	Introduction	1-1
1.2	Report Summary	1-2
2.	GENERAL PROPERTIES OF SIGNALS REFLECTED FROM THE EARTH	2-1
2.1	Specular Reflection	2-1
2.2	Diffuse Scattering	2-11
2.3	Multipath Model	2-19
3.	AIRCRAFT/SYNCRONOUS SATELLITE RELAY	3-1
3.1	Expected Magnitude of Multipath	3-1
3.2	Time and Frequency Dispersion	3-13
3.3	Channel Transfer Function	3-18
4.	WEATHER SATELLITE/SYNCHRONOUS SATELLITE RELAY	4-1
4.1	Expected Magnitude of Multipath	4-1
4.2	Time and Frequency Dispersion	4-8
4.3	Channel Transfer Function	4-10
5.	ANTICIPATED ELECTROMAGNETIC INTERFERENCE	5-1
5.1	Noise	5-1
5.2	External Interference	5-1
5.3	System Internal Interference	5-5
6.	PERFORMANCE OF DIGITAL MODULATION	6-1
6.1	Binary PSK	6-1
6.2	Spread Systems	6-5
6.3	A Fundamental Choice	6-7

CONTENTS -- Continued

Section		Page
6.4	Possible Hybrid System	6-9
7.	PERFORMANCE OF ANALOG VOICE MODULATION	7-1
7.1	AM	7-1
7.2	FM	7-5
8.	REFERENCES	8-1

ILLUSTRATIONS

Figure		Page
2-1	Dependence of the Scattering Coefficient on the Phase Variance. Source: Beckmann and Spizzichino,[3] Figure 14.1	2-3
2-2	Specular Signal Strength for Various Values of Roughness for a 300 Nautical Mile Satellite to a Synchronous Altitude Satellite. Source: Jenny and Weiss,[2] Figure 2-8	2-5
2-3	Reliability for Two-Ray Fading Model ($K=20 \log_{10} k$)	2-7
2-4	Computation of Specular Component From Experimental Data Using R_{10}/R_{90}	2-8
2-5	Computation of Specular Component From Experimental Data Using S_{MAX}/S_{MIN}	2-10
2-6	The Rayleigh Distribution	2-12
2-7	Comparison of Theoretical and Experimental Data for Diffuse Scattering. Source: Beckmann and Spizzichino,[3] Figure 15.3.	2-14
2-8	Distribution of the Amplitude of a Constant Vector Plus a Rayleigh-Distributed Vector. K=Power in Rayleigh Component Relative to Power in Constant Component	2-16
2-9	Computation of Diffuse Component From Experimental Data Using R_{10}/R_{90}	2-18
2-10	Example of Multipath Channel Transfer Function	2-22
3-1	Relative Multipath Power for Aircraft/Synchronous Satellite Data Relay ($\sigma = 1.0$, $T = 10$)	3-3
3-2	Relative Multipath Power for Aircraft/Synchronous Satellite Data Relay ($\sigma = 0.5$, $T = 10$)	3-4

ILLUSTRATIONS -- Continued

Figure		Page
3-3	Relative Multipath Power for Aircraft/Synchronous Satellite Data Relay (σ =1.0, T = 100)	3-5
3-4	Probability Distribution of Signal Fading. Source: Bergemann and Kucera[11] Figure 15.	3-6
3-5	Total Multipath Power of Runs 1, 2 and 3 Compared With Experimental Data	3-8
3-6	Resultant Signal Distributions for Aircraft/Synchronous Satellite (Incidence Angles 0 to 60 Degrees)	3-10
3-7	Resultant Signal Distributions for Aircraft/Synchronous Satellite (Incidence Angle = 70 Degrees)	3-12
3-8	Resultant Signal Distribution for Aircraft/Synchronous Satellite (Incidence Angle = 80 Degrees)	3-14
3-9	Range of Possible Multipath Delays for Aircraft/Synchronous Satellite Relay (Aircraft Altitude = 10 Kilometers	3-16
3-10	Frequency Spreading for Aircraft/Synchronous Satellite Relay: Source Jordan[13].	3-17
3-11	Typical Transfer Function for Aircraft/Synchronous Satellite Relay for Incidence Angles (0 thru 60 Degrees)	3-21
3-12	Typical Transfer Function for Aircraft/Synchronous Satellite Relay for Incidence Angle = 70 Degrees	3-22
3-13	Typical Transfer Function for Aircraft/Synchronous Satellite Relay for Incidence Angle = 80 Degrees	3-23
4-1	Relative Multipath Power for Weather Satellite/Synchronous Satellite Data Relay (σ =1.0, T = 10.0)	4-2

ILLUSTRATIONS -- Continued

Figure		Page
4-2	Relative Multipath Power for Weather Satellite/Synchronous Satellite Data Relay ($\sigma = 0.5$, $T = 10.0$)	4-3
4-3	Relative Multipath Power for Weather Satellite/Synchronous Satellite Data Relay ($\sigma = 1.0$, $T = 100.0$)	4-4
4-4	Resultant Signal Distributions for Weather Satellite/Synchronous Satellite (Incidence Angle=0 Through 70 Degrees)	4-6
4-5	Resultant Signal Distribution for Weather Satellite/Synchronous Satellite (Incidence Angle = 80 Degrees)	4-7
4-6	Range of Possible Multipath Delays for Weather Satellite/ Synchronous Satellite Relay	4-9
4-7	Difference in Doppler Frequencies Between Direct and Reflected Paths for 136 MHz Carrier	4-11
4-8	Bandwidth of Scattered Signal for 136 MHz Carrier Frequency Source: Durrani and Staras.[15]	
4-9	Typical Multipath Channel Transfer Function for Weather Satellite/ Synchronous Satellite Relay (Incidence Angles 0 Through 60 Degrees)	4-14
4-10	Typical Multipath Channel Transfer Function for Weather Satellite/ Synchronous Satellite Relay (Incidence Angle = 70 Degrees)	4-15
4-11	Typical Multipath Channel Transfer Function for Weather Satellite/ Synchronous Satellite Relay (Incidence Angle=80 Degrees)	4-16
5-1	Expected External Interference for TDRS at 110°W Longitude	5-2
5-2	Expected External Interference for TDRS at 143°W Longitude	5-3
7-1	Output Distortion of FM With Specular Reflection at Worst Phasing; Source: Medhurst[25]	7-6

TABLES

Table		Page
1-1	Summary of Multipath Values	1-2
3-1	Median Power in Random Component Relative to Direct Path (dB).	3-9
3-2	Summary of Aircraft/Synchronous Satellite Analysis (All dB Values are Relative to Direct Path Signal Level; Results Based on $\sigma = 1$, $T = 100$)	3-15
3-3	Mean Power of Multipath Components of Figure 3-3 (Aircraft/ Synchronous Satellite)	3-20
4-1	Summary of Weather Satellite/Synchronous Satellite Analysis (All dB Values are Relative to Direct Path Signal Level)	4-8
4-2	Mean Power of Multipath Components of Figure 4-3 (Weather Satellite/Synchronous Satellite Relay)	4-13
6-1	Performance of PSK	6-5
6-2	Performance of Spread Spectrum	6-8
6-3	Required Signal-to-Noise Ratio for MPSK With $P_e = 10^{-5}$	6-11
6-4	Performance of Hybrid System	6-11

COMMUNICATION PERFORMANCE OVER THE TDRS MULTIPATH/INTERFERENCE CHANNEL

1. INTRODUCTION AND SUMMARY OF RESULTS.

1.1 Introduction.

A prime mission of the Tracking and Data Relay Satellite (TDRS) is to relay low- to medium-rate data and/or analog voice from a low altitude platform to an earth station.[1] One of the frequency bands of interest is VHF. Unfortunately, the VHF channel is plagued by both multipath (from the earth) and interference. A previous ESL report developed models for both the multipath and the interference.[2] In this report we apply the models to predict communication system performance for two cases: an aircraft/TDRS and a weather satellite/TDRS relay. The work reported here documents one task assigned to ESL under NASA contract NAS5-20228 and carried out between February 1971 and August 1971.

Section 2 serves as a review of the properties of multipath from the earth. These properties are then applied to the two cases of interest: aircraft relay in Section 3 and weather satellite relay in Section 4. The properties that are summarized include the magnitude of multipath (both specular and diffuse), the differential time delay and doppler shift, and the time and doppler spread. All of these properties are needed to predict communication performance. In addition, we must specify the interference that is expected to be encountered; this is done in Section 5. Having established the

1.1 -- Continued.

properties of the channel, the communications performance is analyzed: digital data in Section 6 and analog voice in Section 7.

1.2 Report Summary.

The properties of the multipath for the two cases under consideration are summarized in Table 1-1. We have entered only those properties of prime interest to communications signal design in Table 1-1. Furthermore, these are maximum values and the reader is cautioned that the maximum values do not all coincide at the same incidence angles. The values as a function of incidence angle are given in the text; Figures 3-3, 3-9, and 3-10 for the aircraft case and Figures 4-3, 4-6, 4-7, and 4-8 for the weather satellite case.

Table 1-1. Summary of Multipath Values

Parameters	Value	
	Aircraft Application	Weather Satellite Application
Specular Magnitude	-9 dB	-18 dB
Diffuse Magnitude	-15 dB	-22 dB
Differential Delay	0.067 msec	7.3 msec
Delay Spreading	2.4 msec	26.0 msec
Differential Doppler	0.1 Hz	750 Hz
Doppler Spreading	50 Hz	1500 Hz

1.2 -- Continued.

We have estimated the external interference from earth-based transmitters as 20 dB greater than thermal noise at the frequencies where interference is present. However, we also point out that there should be on the order of 300 to 400 kHz of interference free spectrum in the 2 MHz bandwidth from 136 to 138 MHz. Other frequency bands can be expected to have the same magnitude of interference but probably fewer slots that are free of interference.

In our analysis of digital modulation we point out that there is a fundamental choice between interference avoidance and multipath avoidance. Interference avoidance is achieved by using relatively narrow bandwidths and controlling frequency assignments to use interference free spectrum. This technique will allow the use of 15 to 20 dB lower effective radiated power in the platforms using the TDRS. However, careful frequency control will be required and the system will not work if the interference free spectrum proves to be an illusion or if the multipath is much more severe than anticipated. Multipath avoidance is achieved by using spread spectrum to reject the multipath. This method must accept the average interference; consequently, the ERP must be raised to counter interference rather than noise. A choice between the two basic methods is difficult at this time owing to the lack of a careful measurement of the electromagnetic environment, particularly the RFI.

Analog voice modulation encounters problems similar to that of digital data. We show that wideband FM (modulation index on the order of two) will outperform both AM and narrowband FM provided that the additional required bandwidth does not force operation into portions of the spectrum with heavy interference.

2. GENERAL PROPERTIES OF SIGNALS REFLECTED FROM THE EARTH.

2.1 Specular Reflection.

Specular reflection is a reflection similar to that from a smooth surface in that it is directional and obeys the laws of classical optics. The reflected energy of the specular component originates in an area on the earth's surface called the first Fresnel zone, which is the area defined by all points on the earth's surface whose path length between transmitter and receiver differs from the minimum time reflection path by less than one-half wavelength of the signal.

The magnitude of the specular reflection is given by $R_s = \rho_s R_o$ where R_o is the reflection coefficient of a smooth spherical earth for a particular earth/satellite geometry and ρ_s is the factor by which R_o must be multiplied to account for the irregularities of the earth's surface. The factor ρ_s is a function of the height of the irregularities, the grazing angle γ between the incoming ray and the surface, and the signal wavelength. To analyze ρ_s quantitatively, suppose that two incoming rays from the same source are reflected: one from the surface and the other from an irregularity of height Δh. Thus, the path difference between the two rays is $2\Delta h \sin \gamma$ and hence the phase difference is

$$\Delta\Phi = \frac{2\pi}{\lambda} (2\Delta h \sin \gamma) = \frac{4\pi\Delta h \sin \gamma}{\lambda} .$$

Lord Rayleigh proposed to consider a surface smooth if

$$\Delta\Phi < \frac{\pi}{2}$$

so that all reflections are from points in the first Fresnel zone. This requires

2.1 -- Continued.

$$\frac{\Delta h}{\lambda} \sin \gamma < \frac{1}{8}$$

This condition can be satisfied if

$$\frac{\Delta h}{\lambda} << 1 \text{ or } \sin \gamma << 1 \ .$$

Thus if the surface irregularities are a small fraction of a wavelength or the grazing angle γ is small, the surface can be considered smooth, which implies $\rho_s = 1$. Beckmann and Spizzichino[3] improved on this approximation by deriving an exact expression for the mean-square value of ρ_s for a Gaussian-distributed surface; i.e.,

$$<|\rho_s|^2> = \exp\left[\frac{-4\pi\Delta h \sin\gamma}{\lambda}\right]^2$$

where γ and λ are the same as above and Δh is the standard deviation of the Gaussian surface distribution. This expression is plotted in Figure 2-1 along with experimental data. The deviation of the experimental data for $\Delta\Phi > 0.4\pi$ is apparently due to diffuse scattering which was not separated from the specular reflection in the experiment.

The Rayleigh criterion ($\Delta\Phi < \pi/2$) then implies $<|\rho_s|^2> > 0.08$ or $(\rho_s)_{rms} > 0.28$. Thus if the Rayleigh criterion is satisfied in a given situation, the rms value of ρ_s is at least 0.28, and the actual value can be estimated using Figure 2-1. For example, if $\Delta h = 0.1\lambda$ and $\gamma = 30°$, then

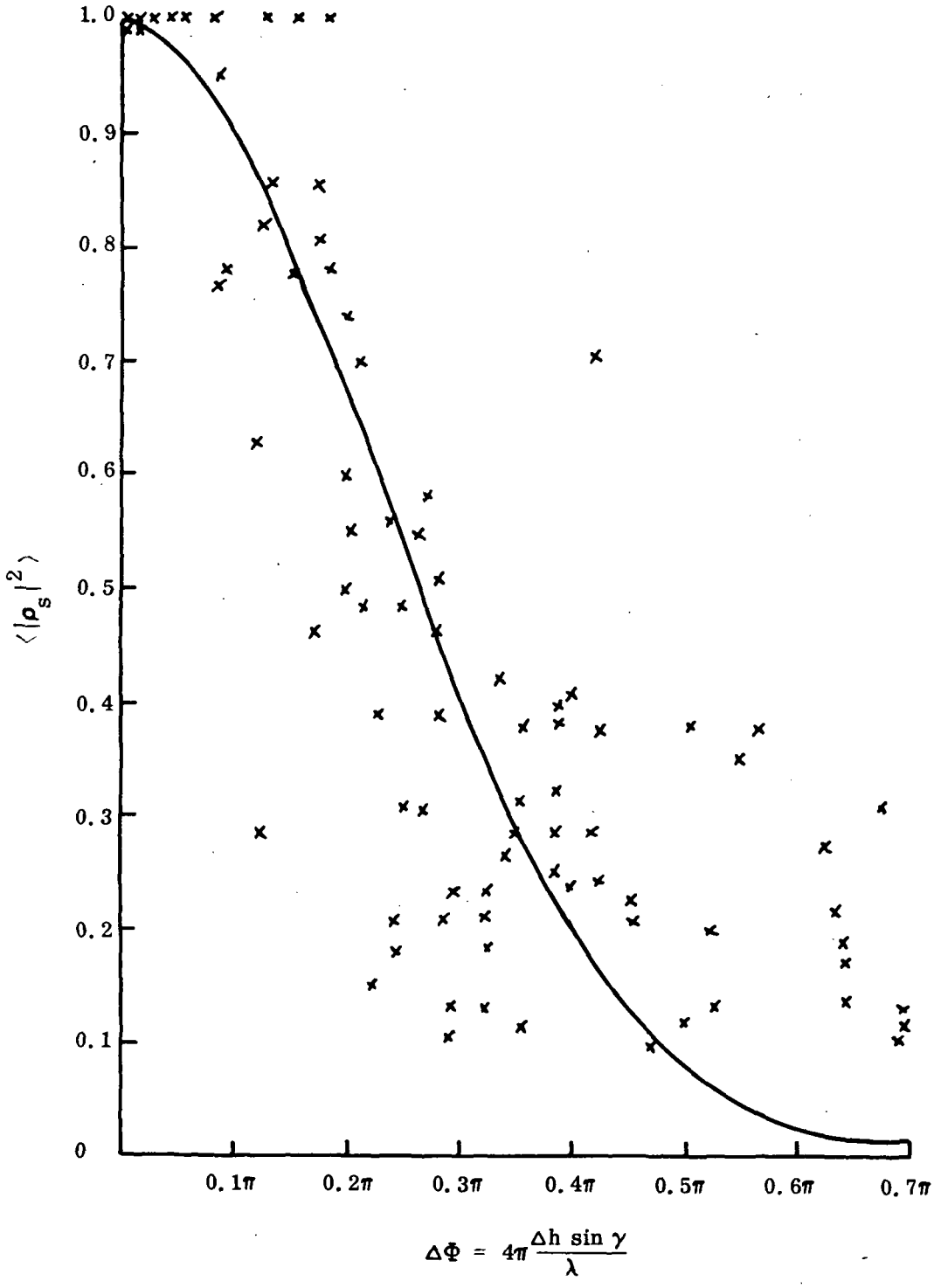

Figure 2-1. Dependence of the Scattering Coefficient on the Phase Variance. Source: Beckmann and Spizzichino,[3] Figure 14.1

2.1 -- Continued.

$$\Delta\Phi = \frac{4\pi\,(0.1\lambda)\,\sin 30^\circ}{\lambda} = 0.2\pi$$

From Figure 2-1, $< |\rho_s|^2 > = 0.66$ and $(\rho_s)_{rms} = 0.81$.

Although the specular component of the multipath is generally considered to be constant with time, fluctuations can occur due to changes in the roughness and reflectivity of the terrain caused by motion of the transmitter and/or receiver platforms. As the reflection point passes over smooth surfaces the specular reflection becomes large while passage over rough surfaces can cause the reflection to disappear (see Figure 2-2).

The direct path signal at the receiver can be represented by

$$S_o(t) = V \sin \omega t$$

The signal at the receiver due solely to specular reflection (assuming no differential doppler shift) can be represented as

$$S_R(t) = kV \sin (\omega t + \phi)$$

where k is constant such that $0 \leq k \leq 1$ and ϕ is the relative phase shift due to the differential path delay. The total received signal is thus given by

$$S_T(t) = S_o(t) + S_R(t) = V\,[\sin \omega t + k \sin (\omega t + \phi)\,]$$

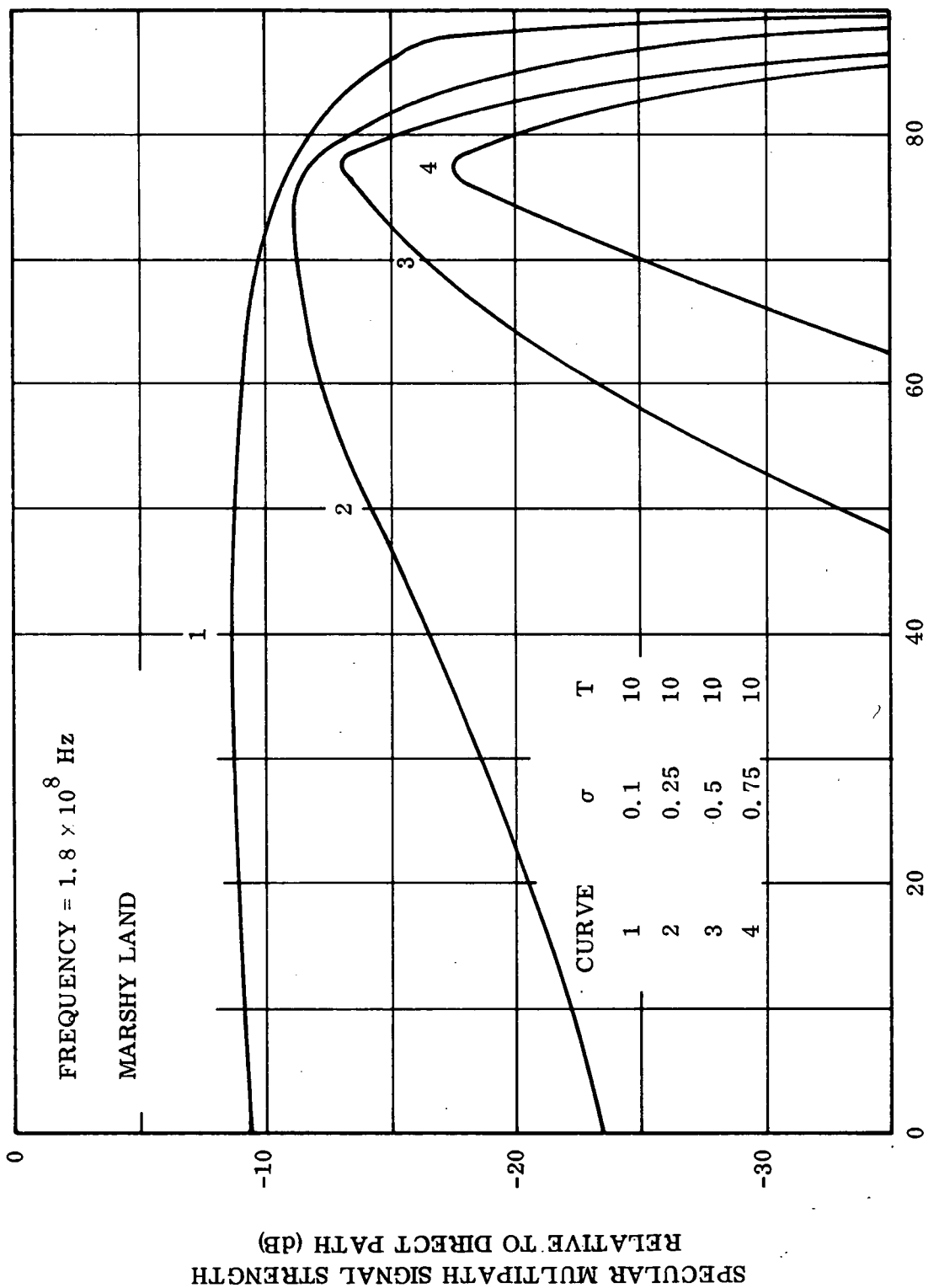

Figure 2-2. Specular Signal Strength for Various Values of Roughness for a 300 Nautical Mile Satellite to a Synchronous Altitude Satellite. Source: Jenny and Weiss,[2] Figure 2-8

2.1 -- Continued.

Since ϕ can take on any value between zero and 2π we can regard it as being uniformly distributed over zero to 2π. The probability density of the envelope R of $S_T(t)$ was derived by Slack[4] and is given by

$$p(R) = \frac{2R}{\pi}\left[\left(2kV^2\right)^2 - \left(R^2 - [1+k^2]^2 V^2\right)^2\right]^{-\frac{1}{2}}$$

where $(1-k)V \leq R \leq (1+k)V$. The probability distribution is thus obtained

$$F(R) = \int_0^R p(u)\, du$$

$$= \frac{1}{\pi}\cos^{-1}\left[\left(1+k^2 - (R/V)^2\right)/2k\right]$$

The complement of F(R), i.e., $[1-F(R)]$ yields the reliability, which is plotted in Figure 2-3. Notice that the fading distributions are relatively flat for high probabilities, owing to the fact that the minimum envelope level is limited by the model to (1-k)V.

The magnitude of the specularly reflected component in dB, i.e., $K = 20 \log_{10} k$ can be computed from experimental data by determining the ratio of the amplitude of the resultant exceeded for 10 percent of the time to the amplitude of the resultant exceeded for 90 percent of the time, i.e., R_{10}/R_{90}. A curve for determining K from this ratio can be derived directly from Figure 2-3 and is shown in Figure 2-4.

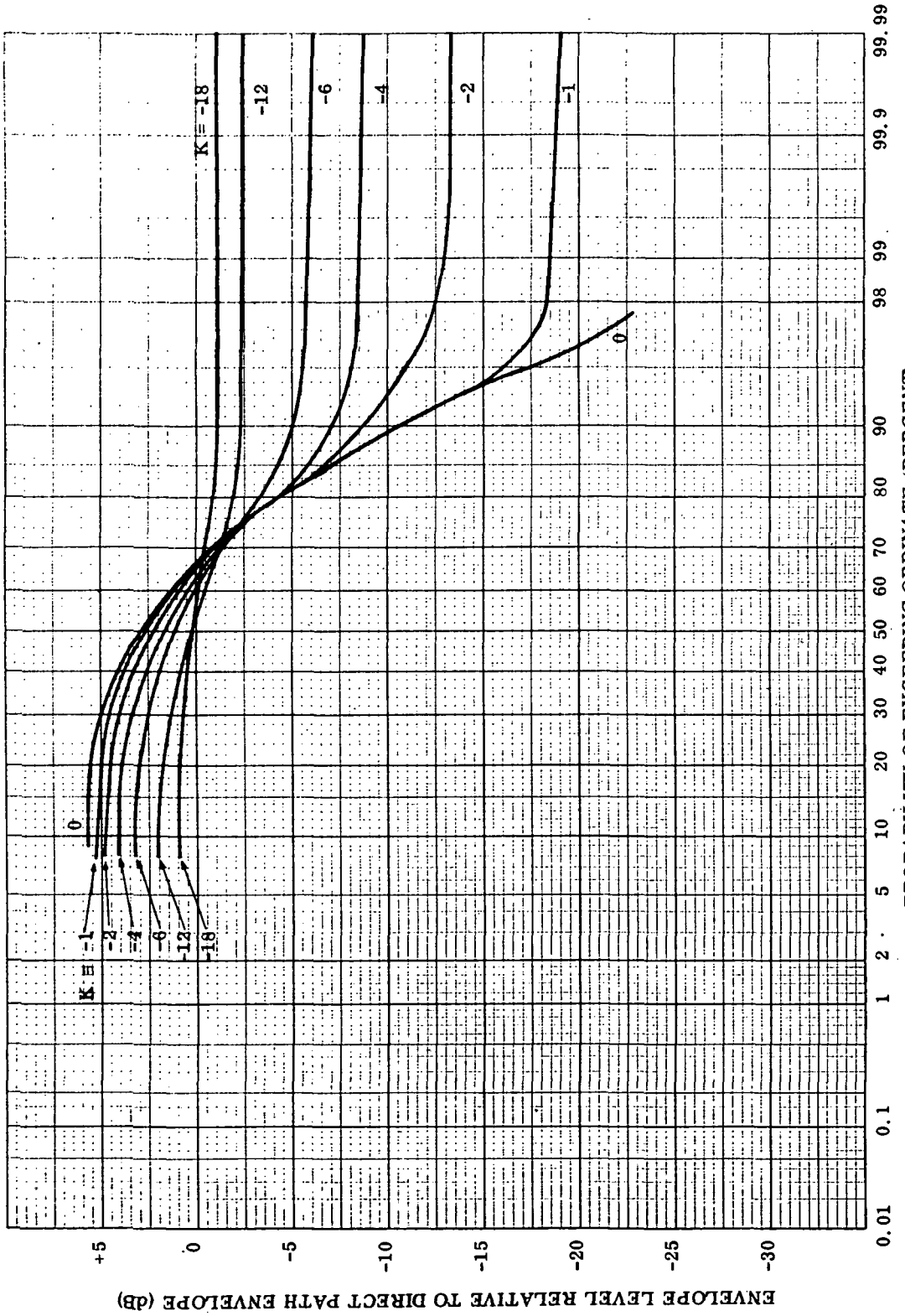

Figure 2-3. Reliability for Two-Ray Fading Model ($K = 20 \log_{10} k$)

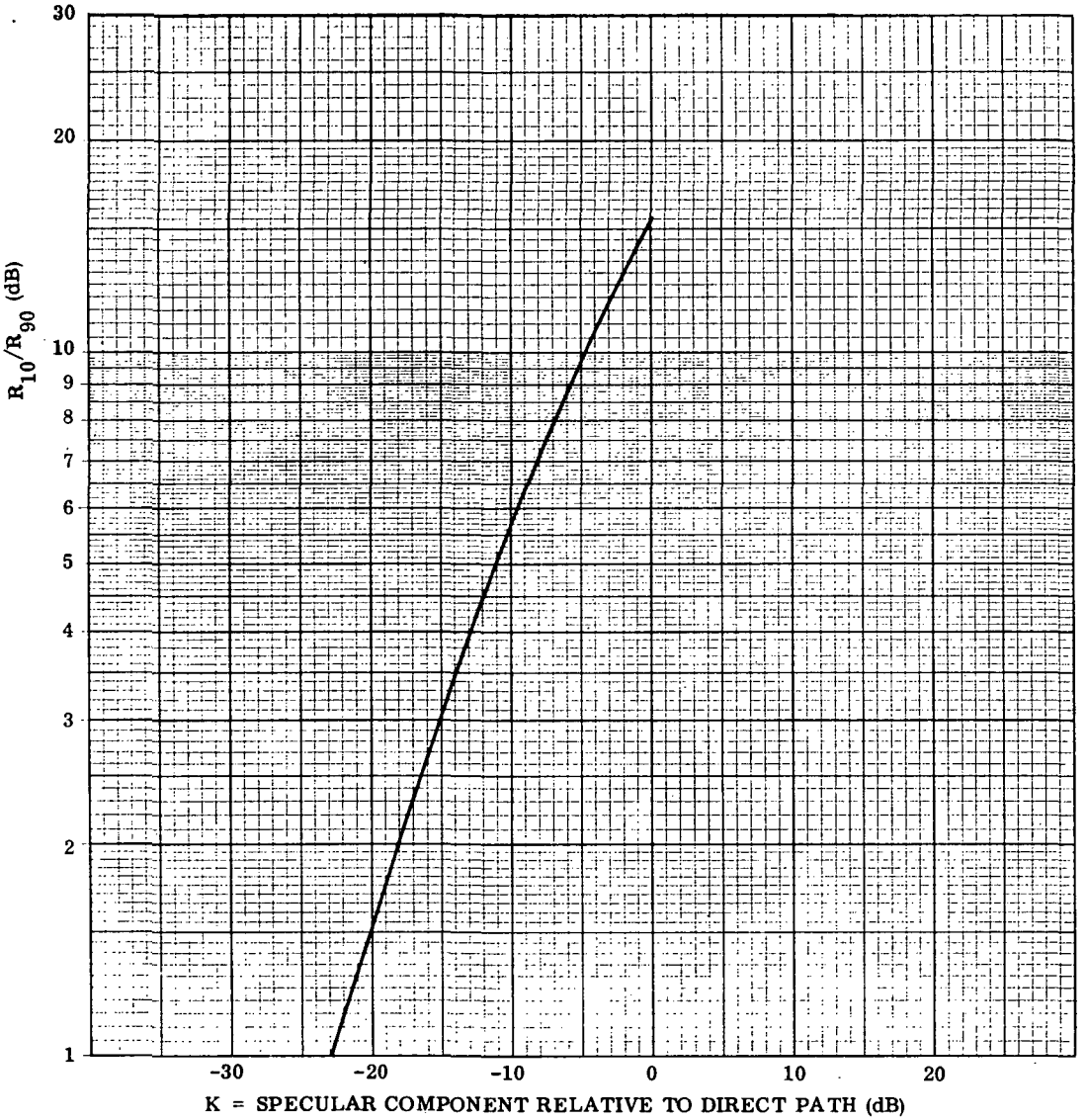

Figure 2-4. Computation of Specular Component From Experimental Data Using R_{10}/R_{90}

2.1 -- Continued.

For example suppose that for a certain group of collected data + 10 dB relative to a reference signal level is exceeded 10 percent of the time and +1 dB relative to the same reference is exceeded 90 percent of the time. Therefore, R_{10}/R_{90} = 10 dB -1 dB = 9 dB and from Figure 2-4 the value of K obtained is -6 dB.

If the fading caused by the specular component is very regular, the magnitude of $K = 20 \log_{10} k$ can be determined from the minimum and maximum values of the resultant signal, i.e., $S_{MAX} = V(1+k)$ and $S_{MIN} = V(1-k)$.

$$\frac{S_{MAX}}{S_{MIN}} = \frac{1 + k}{1 - k}$$

and

$$k = \frac{S_{MAX}/S_{MIN} - 1}{S_{MAX}/S_{MIN} + 1} \qquad (2\text{-}1)$$

Thus, by measuring S_{MAX}/S_{MIN}, the magnitude of the specular component K can be determined. Equation (2-1) is plotted in Figure 2-5 for this purpose. For example, if S_{MAX}/S_{MIN} = 8 dB, then K = -7 dB.

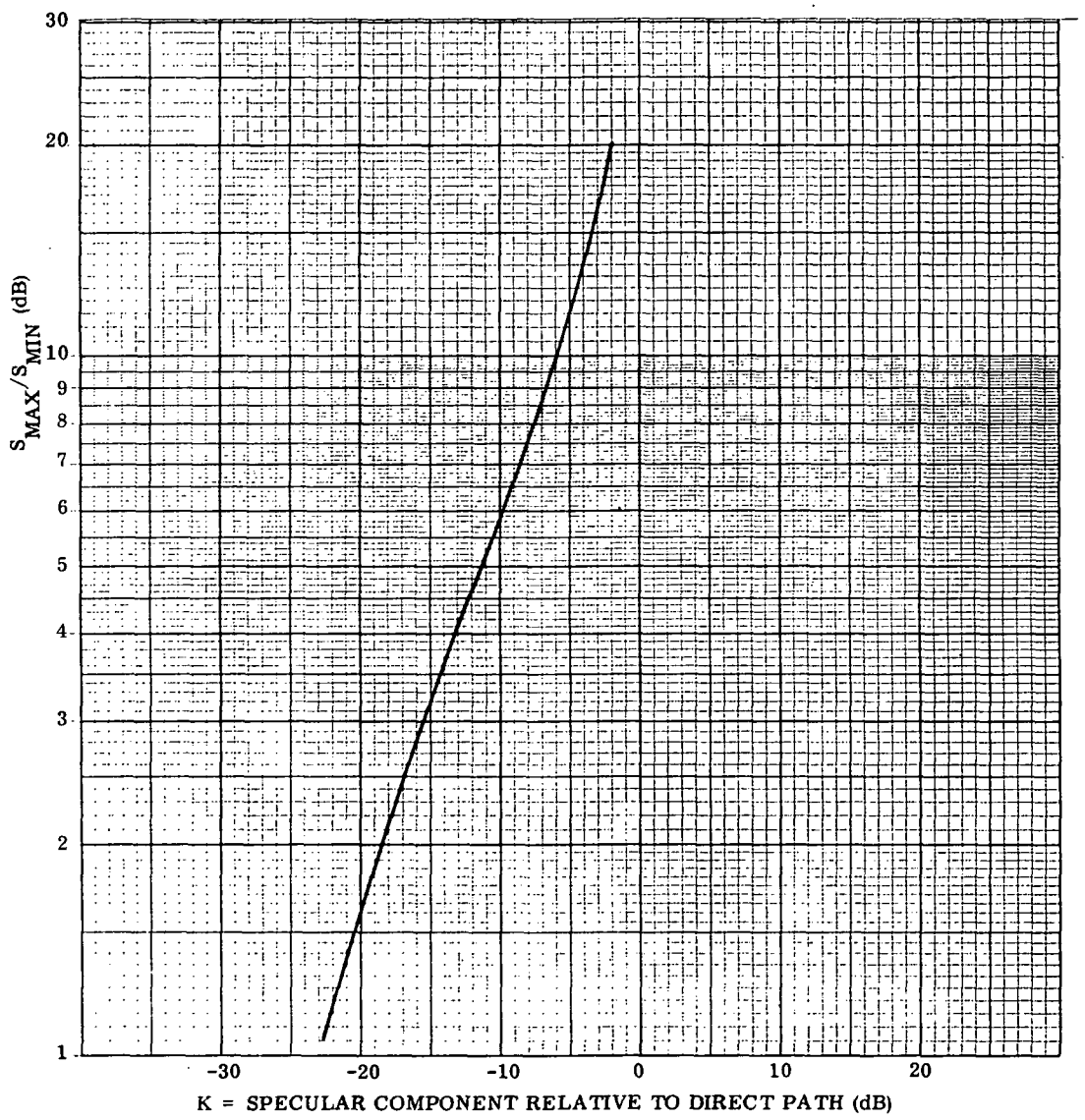

Figure 2-5. Computation of Specular Component From Experimental Data Using S_{MAX}/S_{MIN}

2.2 Diffuse Scattering.

As previously defined, the diffuse multipath component is reflected from the remainder of the earth (outside the first Fresnel zone) which is within line-of-sight of both transmitter and receiver. As stated by Beckmann and Spizzichino[3] the amplitude of the diffuse multipath component is Rayleigh distributed. To see how this result is described physically, consider a large number of interfering signals which are reflected from the earth to the receiver by the process of diffuse scattering. Owing to the large surface area from which the signals are reflected and the surface roughness, the reflected signals have essentially random amplitudes and uniformly distributed phases. As described in Schwartz, Bennett, and Stein, as few as six equal amplitude sine waves with independently fluctuating random phases will yield a resultant whose envelope is Rayleigh distributed and whose phase is uniformly distributed.[5] The Rayleigh distribution can be completely specified by one parameter, the mean square signal (or average power), such that

$$P\left\{\frac{R^2}{\overline{R^2}} > u\right\} = \exp\left[-u^2\right] \qquad (2\text{-}2)$$

as shown in Figure 2-6. This expression is plotted in terms of probability (in percent) that the ratio of the signal squared to the mean squared signal exceeds a given level u in dB. Note that if u = 1, then $P\{R^2 > \overline{R^2}\} = \exp[-1] = 37$ percent, so that the mean power is exceeded 37 percent of the time for a Rayleigh distribution.

The use of average power is particularly convenient since Beckmann and Spizzichino[3] and the ESL multipath prediction model[2] both determine average power quantities.

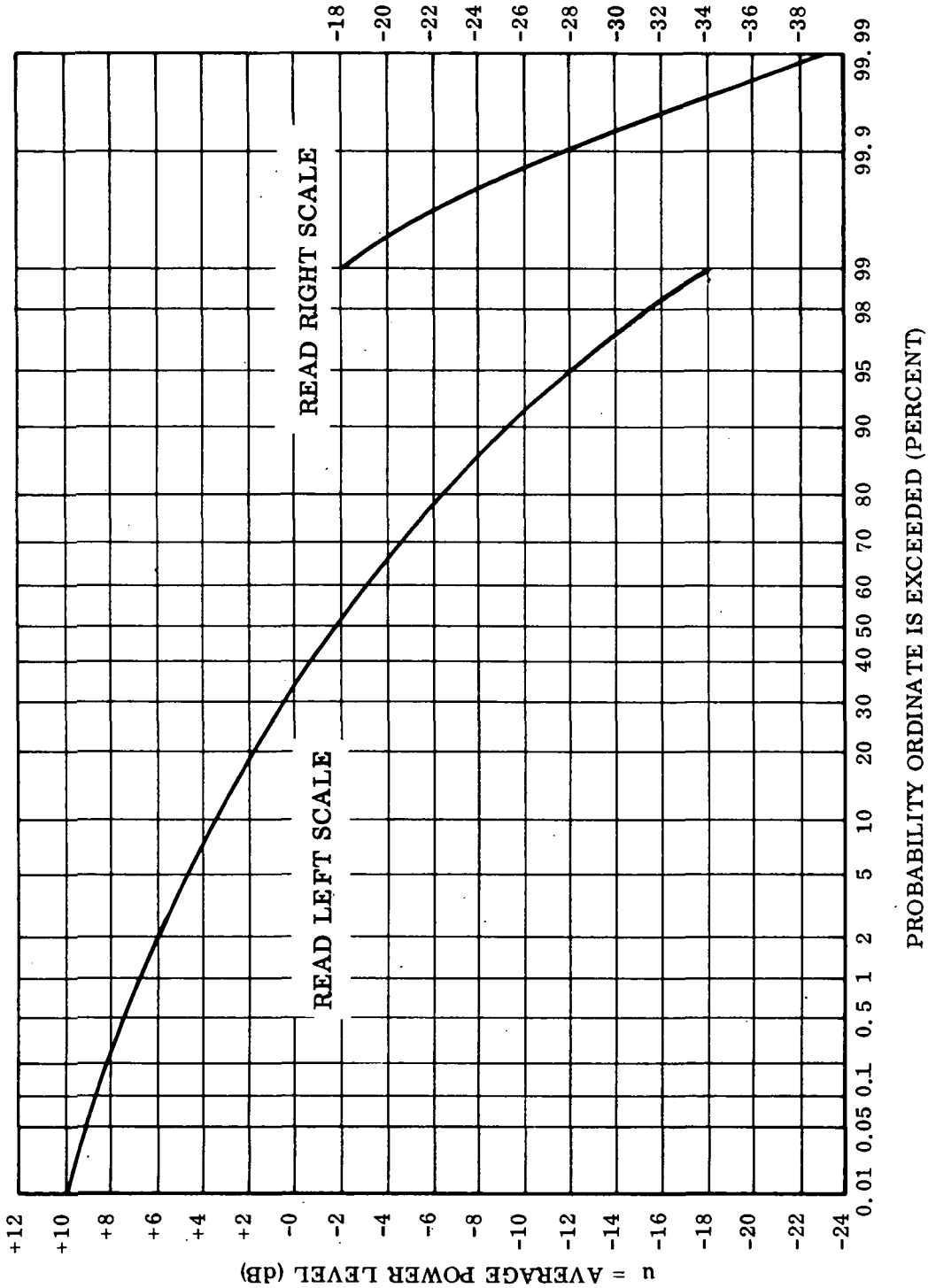

Figure 2-6. The Rayleigh Distribution

2.2 -- Continued.

Finally, it should be noted that the vector sum of two or more independent Rayleigh-distributed vectors is also a Rayleigh-distributed vector, and the mean power from the sum of two or more Rayleigh-distributed vectors is equal to the sum of the mean powers available from each of them. Thus, even if we have Rayleigh-distributed vectors arising from essentially separate regions of the earth, the resultant is still Rayleight-distributed.

The magnitude of the multipath component due to diffuse scattering is given by $R_d = \rho_d . R_o$ where R_o is the reflection coefficient of a smooth spherical earth for a particular earth/satellite geometry and ρ_d is the factor by which R_o must be multiplied to account for the irregularities of the earth's surface. The magnitude of the reflection coefficient R_o depends upon the earth/satellite geometry, which includes the effects of path loss, and the area of the reflecting surface seen by both transmitter and receiver platforms.

Detailed experiments have been performed in order to measure ρ_d [Beckmann and Spizzichino] and indicate that generally speaking ρ_d does not depend on the path geometry, the surface irregularities, or the signal wavelength. Experimental results indicate that the value of ρ_d lies between 0.2 and 0.4 with a probable value of 0.35. By using $\rho_d = 0.35$ and assuming that the sum of the specularly reflected and diffusely scattered energy is constant, the theoretical curve of ρ_d can be compared with experimental results as shown in Figure 2-7. Thus ρ_d is essentially constant, provided the Rayleigh criterion $\Phi < \pi/2$ is not satisfied.

As described previously, the diffusely scattered component is Rayleigh distributed in amplitude and uniformly distributed in phase. The resultant obtained by combining

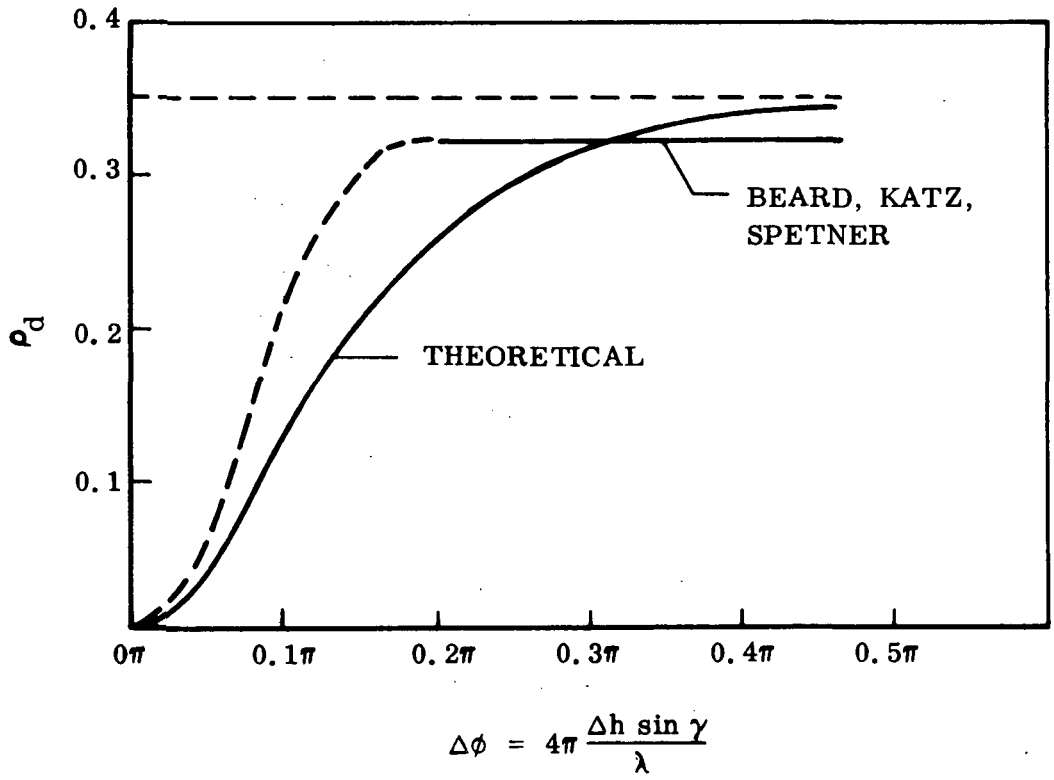

Figure 2-7. Comparison of Theoretical and Experimental Data for Diffuse Scattering. Source: Beckmann and Spizzichino,[3] Figure 15.3

2.2 -- Continued.

such a Rayleigh-distributed vector with a constant vector is known as the Rice distribution.[6] In this case the resultant received signal is of the form

$$S_T(t) = V\,[\sin \omega t + k(t) \sin (\omega t + \phi)]$$

where k(t) is Rayleigh distributed and ϕ is uniformly distributed over $(0, 2\pi)$. The probability density of the envelope R of S(t) is then given by

$$p(R) = \left(\frac{2R}{\overline{R_d^2}}\right) I_o\left(\frac{2R}{\overline{R_d^2}}\right) \cdot \left[\exp - (1 + R^2) / \overline{R_d^2}\right]$$

where $\overline{R_d^2}$ is the mean-square value (average power) of the diffuse component (assuming the direct path has unity value) and I_o is a modified Bessel function of the first kind of order zero.

Using the above probability density, the reliability can be obtained[7] as shown in Figure 2-8. It should be noted that the phase of the resultant is uniformly distributed only for large K. The value K is the average power in the Rayleigh (diffuse) component in dB relative to the average power in the constant (direct) component. Therefore, the ESL multipath prediction model output for the diffuse component (when the specular component is negligible) is exactly equal to K, so that the resultant signal distribution can be obtained directly from Figure 2-8. For example, if the model predicts K = -8 dB, the resultant signal distribution is given by the -8 dB curve in Figure 2-8, which shows that the resultant will be greater than -3 dB 90 percent of the time.

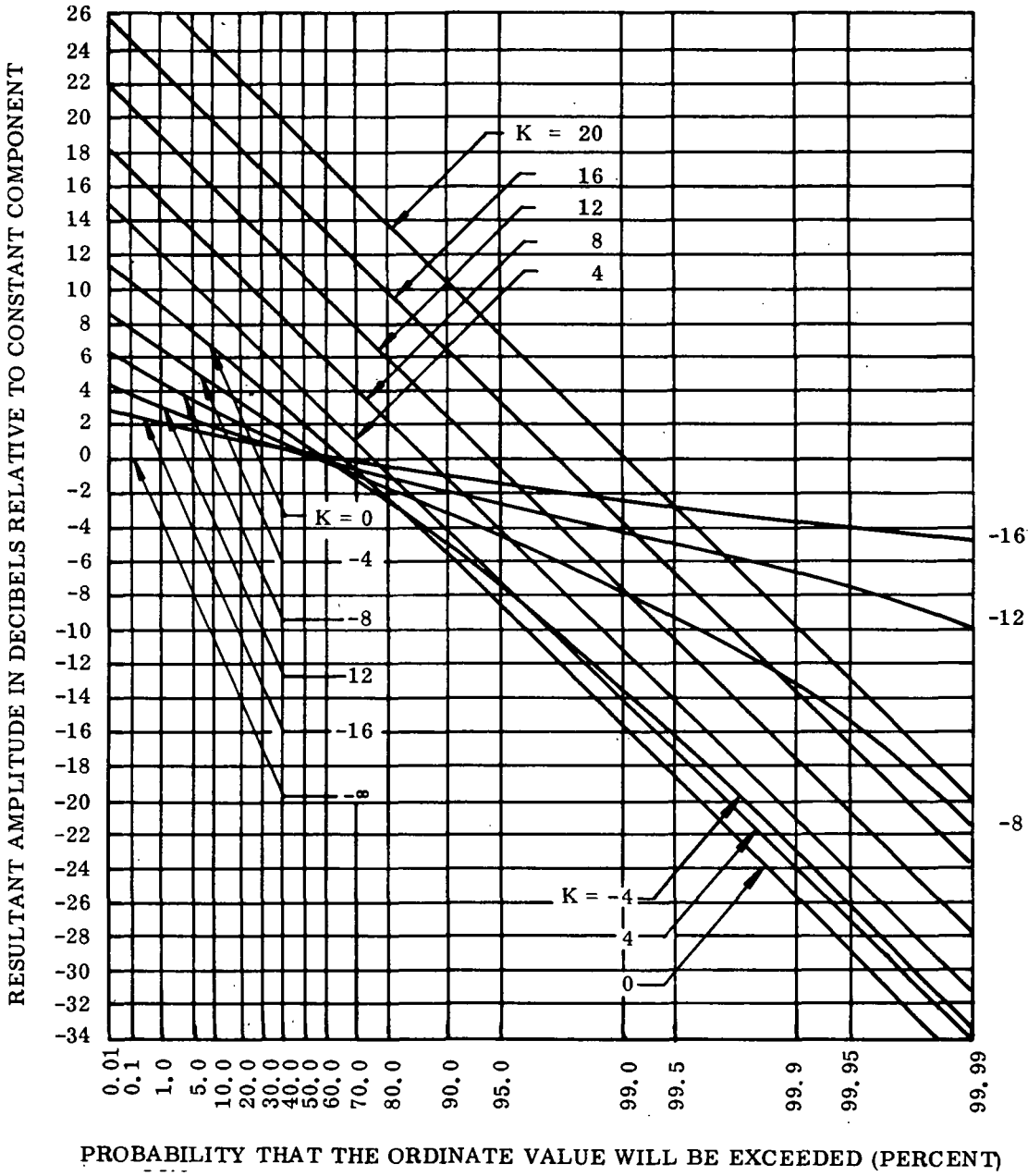

Figure 2-8. Distribution of the Amplitude of a Constant Vector Plus a Rayleigh-Distributed Vector. K = Power in Rayleigh Component Relative to Power in Constant Component

2.2 -- Continued.

The value of K can also be calculated from experimental data by determining the ratio of the amplitude of the resultant exceeded for 10 percent of the time to the amplitude of the resultant exceeded for 90 percent of the time, i.e., R_{10}/R_{90}. A curve for determining K from this ratio can be derived directly from Figure 2-8 and is shown in Figure 2-9. For example, if R_{10}/R_{90} equals 5 dB, then K = -10 dB, and so on.

Polarization effects also enter into diffuse scattering. For specular reflection, the incident wave is not depolarized if it is polarized purely vertical or purely horizontal. Diffuse scattering, on the other hand, is strongly depolarized. Direct measurement of the diffusely scattered component due to a wave transmitted vertically polarized indicates that the scattered field received at horizontal polarization is on the same order as the scattered field received at vertical polarization.[3]

Finally, it is worthwhile to consider the analysis of diffuse scattering if specular reflection is also present. A common approach is to consider the specular component S_s as constant, since it varies more slowly than the diffuse component S_D. Then the problem can be described as the interference of a constant vector $(S_o + S_s)$ with a Rayleigh distributed vector S_D, where S_o is the direct path component.

For example, if a specular component of -6 dB and a diffuse component of -12 dB are received relative to the direct path, then the procedure would first be to combine the specular with the direct path using the two-ray model of Figure 2-3. As shown by this figure, a value of K = -6 dB leads to destructive fading of magnitude -6 dB relative to the direct path or constructive fading of +3 dB relative to the direct path. Thus, the interference of the constant vector (specular plus direct) with the diffuse component will be significantly affected, depending upon the magnitude of the constant vector. If

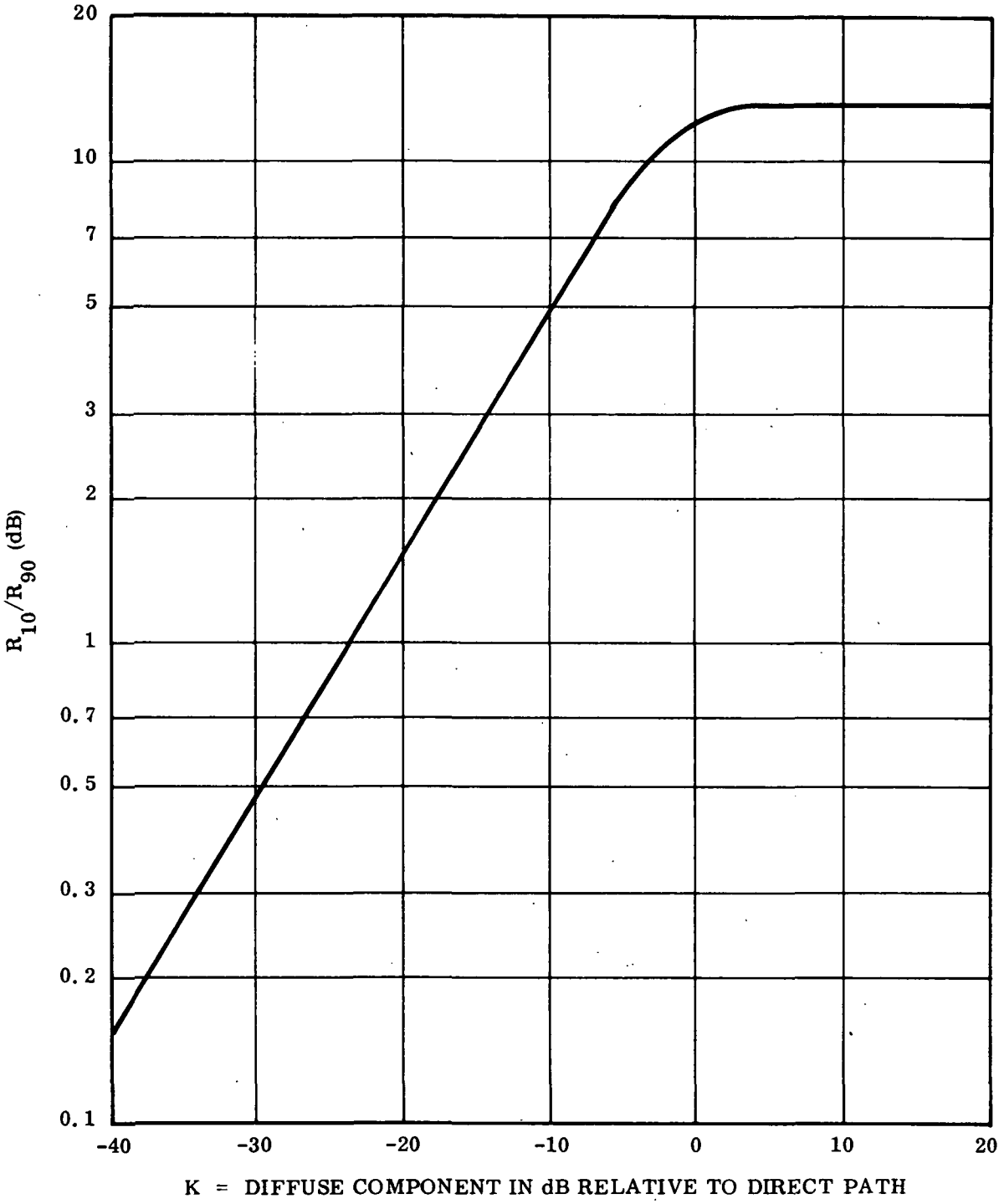

Figure 2-9. Computation of Diffuse Component From Experimental Data Using R_{10}/R_{90}

2.2 -- Continued.

destructive fading occurs, then the ratio of the diffuse component to the constant vector is -12 dB - (-6 dB) = -6 dB. In this case the fading can be described by the K = -6 dB curve in Figure 2-8. If constructive fading occurs, then the ratio is -12 dB - (+3 dB) = -15 dB, so that the fading is described by the K = -15 dB curve in Figure 2-8. Thus, this approach allows us to determine the fading effects due to both specular and diffuse components simultaneously.

2.3 Multipath Model.

A simplified model of the multipath situation described in Sections 2.1 and 2.2 can be obtained by assuming that all multipath components are attenuated and delayed versions of the original transmitted signal. The signal received at a relay satellite is thus given by

$$\underbrace{\widetilde{r(t)}}_{\substack{\text{Total}\\ \text{Received}\\ \text{Signal}}} = \underbrace{s(t)}_{\substack{\text{Direct}\\ \text{Path}}} + \underbrace{\widetilde{k_o s(t-\tau_o)}}_{\substack{\text{Specular}\\ \text{Reflection}}} + \underbrace{\sum_{i=1}^{n} k_i\, s(t-\tau_i)}_{\substack{\text{Diffuse}\\ \text{Scattering}}}$$

2.3 -- Continued.

where k_i = attenuation factor of ith component relative to the direct path signal and τ_i = time delay of ith component relative to direct path signal. Taking the Fourier transform of r(t), we obtain

$$R(f) = S(f)\left\{1 + \sum_{i=0}^{n} k_i \exp\left[-j2\pi f\tau_i\right]\right\}$$

where

$$R(f) = \mathcal{F}\left\{r(t)\right\} \text{ and } S(f) = \mathcal{F}\left\{s(t)\right\} .$$

Therefore, the transfer function for the channel with multipath is

$$H(f) = 1 + \sum_{i=0}^{n} k_i \exp\left[-j2\pi f\tau_i\right] \qquad (2\text{-}3)$$

The values of k_i and τ_i are functions of the satellite geometry and the reflecting properties of the earth. The range of f of interest is limited to the range of S(f), the transmitted signal spectrum. If $2\pi f\tau_i$ undergoes a radian of variation as f varies over the n+1 signal paths, then distortion of the signal spectrum results, because the amplitude and phase relationships of the spectral components of the modulating signal are altered.

2.3 -- Continued.

In the simpler case, when nearly all of the reflected power is in the specular component, then $H(f) = 1+k_o \exp[-j2\pi f \tau_o]$. Therefore, H(f) has a periodic variation in magnitude and phase as f varies over the range of S(f), with the period of the variation equal to $1/\tau_o$ Hz. An example of H(f) for $k_o = 0.5, \tau_o = 65$ microseconds, and f = 130 MHz ±15 kHz is shown in Figure 2-10.

The multipath model described by Equation (2-3) can also be extended to the case of a random channel by choosing the k_i and τ_i from appropriate statistical distributions. Furthermore, doppler can be introduced by allowing different values of frequency for each component. The multipath model then becomes

$$H(f,t) = 1 + \sum_{i=0}^{n} \sum_{\ell=0}^{m} k_{i,\ell} \exp[-j2\pi f \tau_i] \exp[+j2\pi \lambda_\ell t]$$

This is the tapped delay-line model introduced by Kailath[8] and used extensively in the analysis of communication systems; for a survey of results see Daly, Kailath, and Sheft.[9] A continuous version, using integrals in place of summations, is also used.

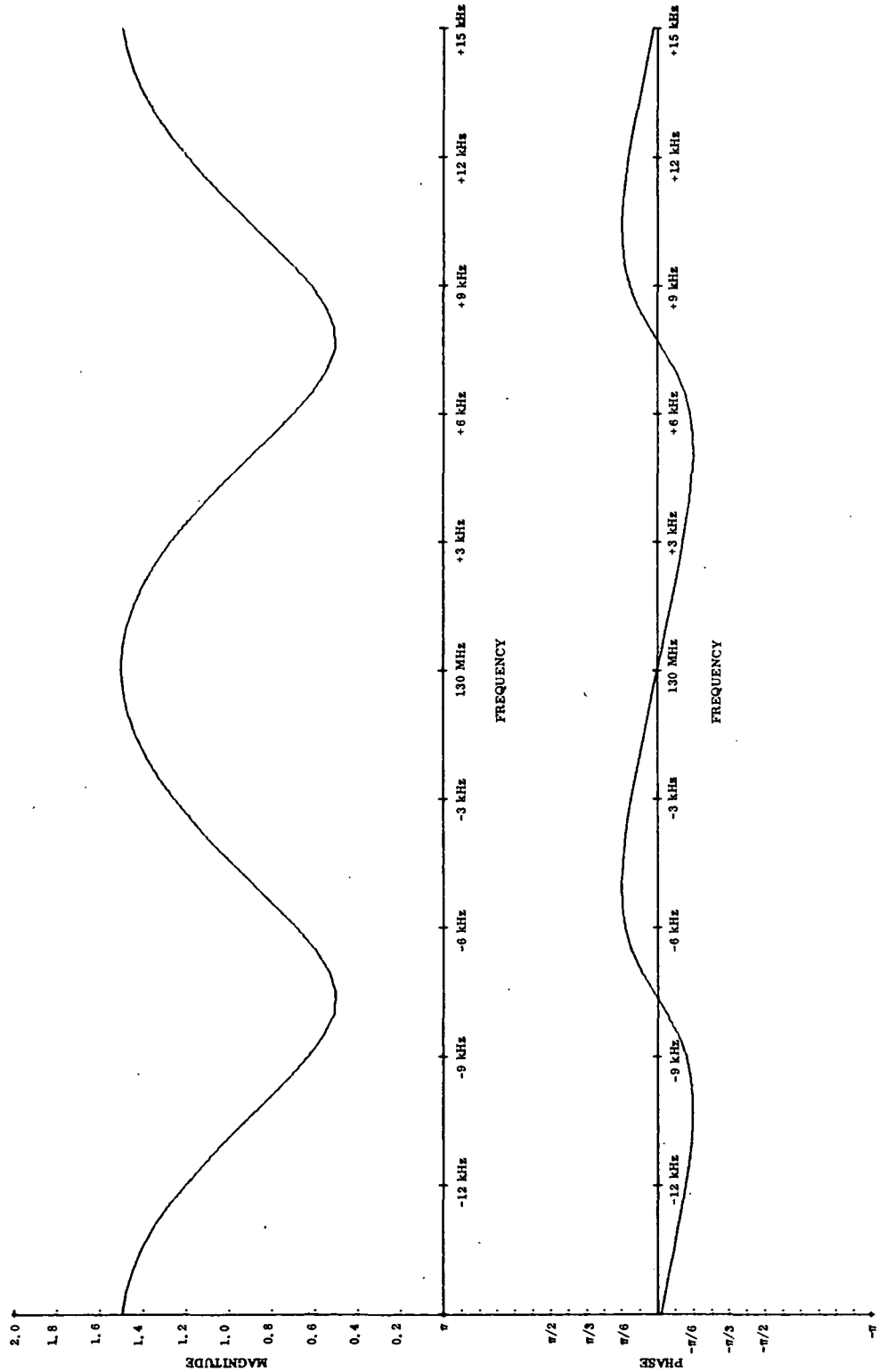

Figure 2-10. Example of Multipath Channel Transfer Function

3. AIRCRAFT/SYNCHRONOUS SATELLITE RELAY.

3.1 Expected Magnitude of Multipath.

In previous work ESL applied the results of Beekmann and Spizzichino to develop a computer model to predict multipath for arbitrary transmitter/receiver/earth geometries, surface parameters, frequencies, and polarization.[10] The model was then used to analyze the effects of geometry and surface parameters on the received multipath signal.[2] One of the findings was that the surface reflectivity does not affect the shape of the specular or diffuse curves, only the magnitudes. For specular reflection, the effect of replacing marshy land as the reflecting surface with sea water is to increase the specular reflection at all angles by about 2.5 dB. Similarly for diffuse scattering, the curves are shifted upward by 3 to 5 dB, depending on surface roughness σ and correlation length T.

The ESL multipath prediction model was applied to the aircraft/synchronous satellite case with the following parameters:

Signal Frequency	=	130 MHz
Aircraft Altitude	=	10 kilometers
Surface Reflectivity	=	Marshland Equivalent

	Surface Roughness (Meters)	Correlation Length (Meters)
Run No. 1	1.0	10.0
Run No. 2	0.5	10.0
Run No. 3	1.0	100.0

3.1 -- Continued.

The results of runs 1, 2, and 3 are shown in Figures 3-1, 3-2, and 3-3, respectively. Several general observations can be made from these figures: 1) the specular component is very sensitive to surface roughness but not to correlation length, 2) the specular component is much less than the diffuse component for incident angles less than 40 degrees (less than 60 degrees for runs 1 and 2), and 3) the diffuse component is nearly constant over all incident angles (especially runs 2 and 3).

In order to determine which of runs 1, 2, and 3 is closest to representing the true situation, these results will be related to experimental data for an aircraft/synchronous satellite data relay reported by Bergemann and Kucera.[11] Their data is reproduced in Figure 3-4, where the angles indicated have been converted to incident angles of the specular component. According to the procedure described previously in Section 2 for determining the magnitude of the multipath signal power, it is necessary to determine the ratio of the signal level which is exceeded 10 percent of the time to the signal level which is exceeded 90 percent of the time. From Figure 3-4, these values are:

$$\text{(20-60 degrees)} \quad R_{10}/R_{90} = 1.5 \text{ dB} - (-1\text{dB}) = 2.5 \text{ dB}$$

$$\text{(60-90 degrees)} \quad R_{10}/R_{90} = 2.0 \text{ dB} - (-2.5\text{dB}) = 4.5 \text{ dB}$$

Next, K, the magnitude of the multipath signal compared with the direct signal can be estimated from Figure 2-4 (two-ray fading model) or Figure 2-9 (Rice fading model).

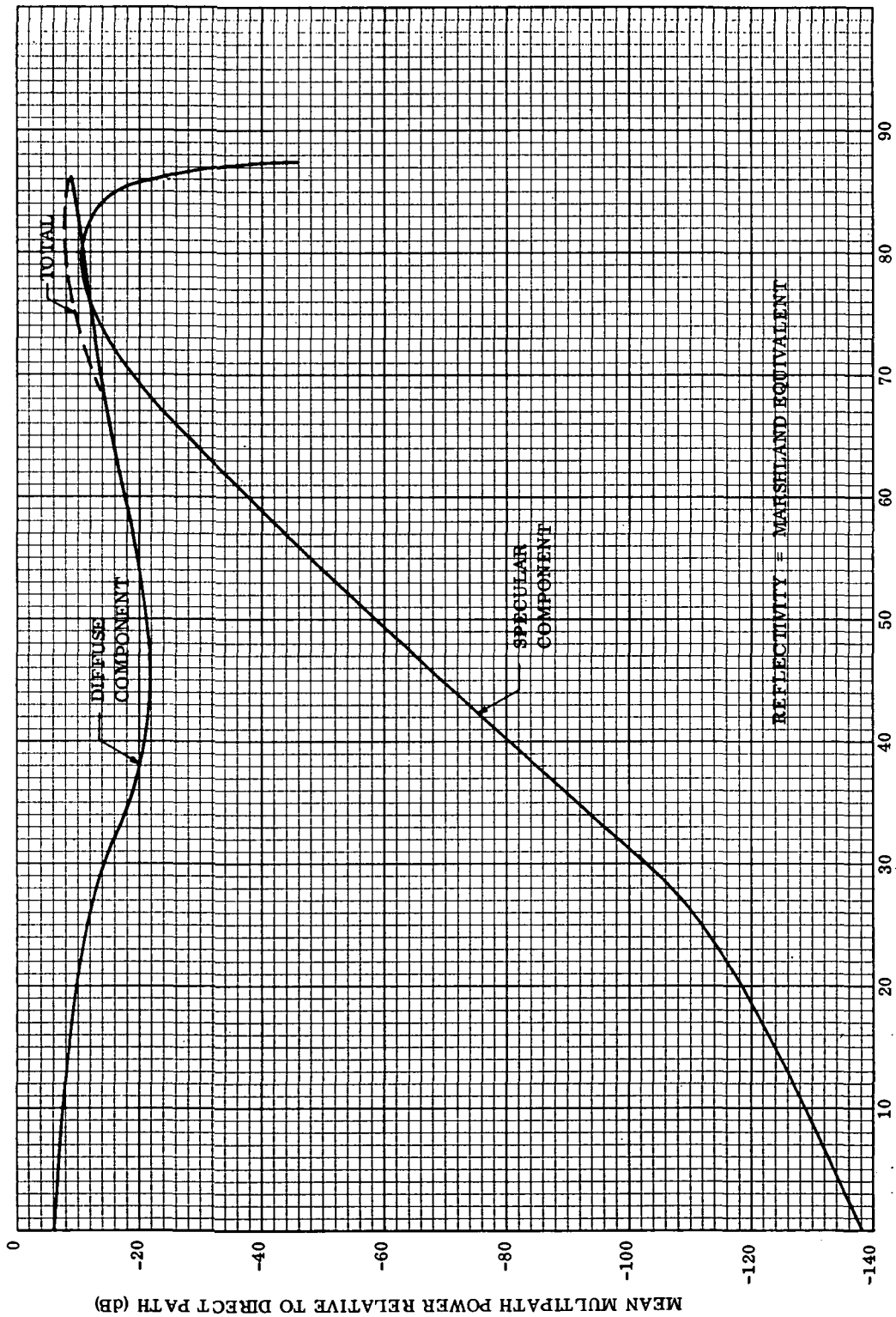

Figure 3-1. Relative Multipath Power for Aircraft/Synchronous Satellite Data Relay (σ = 1.0, T = 10)

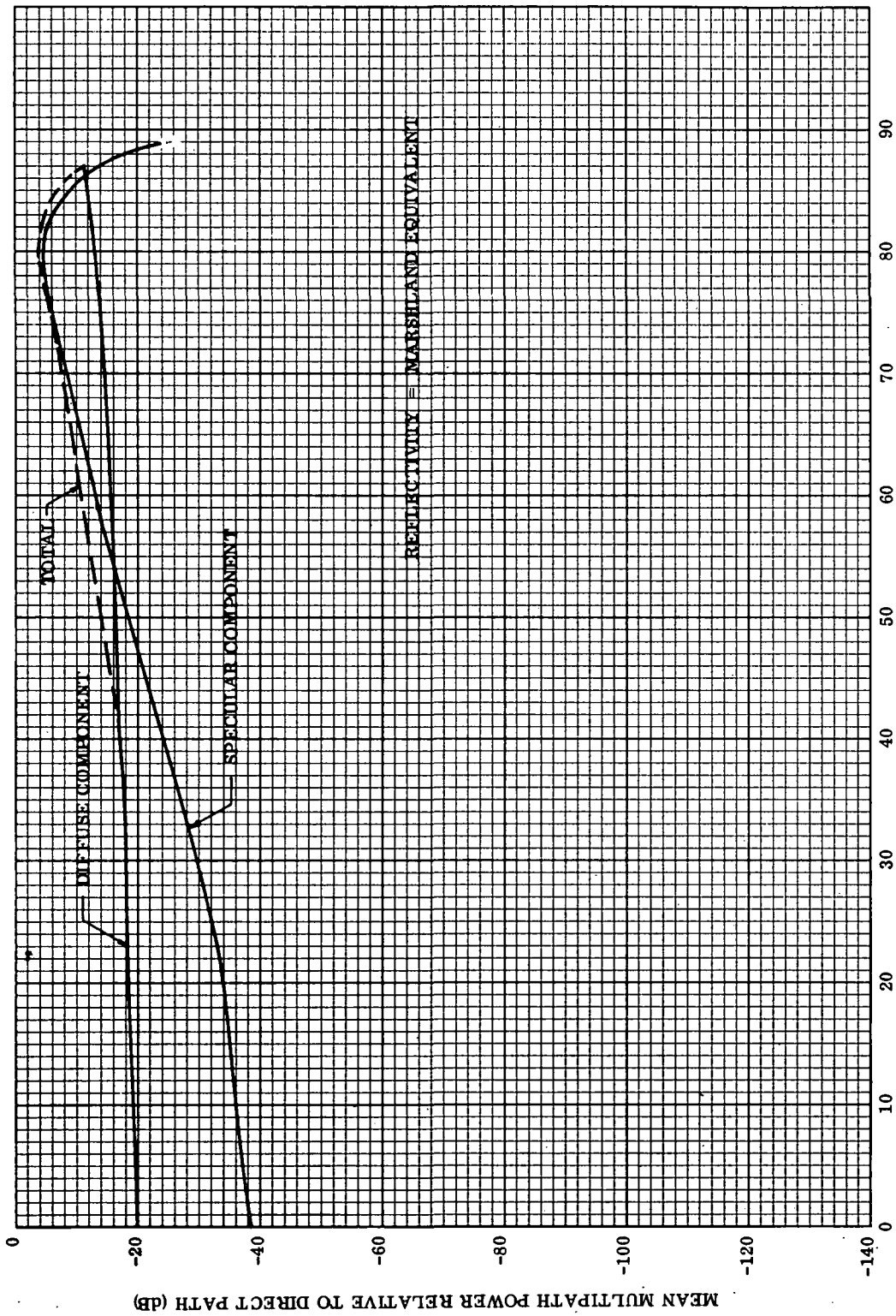

Figure 3-2. Relative Multipath Power for Aircraft/Synchronous Satellite Data Relay (σ = 0.5, T = 10)

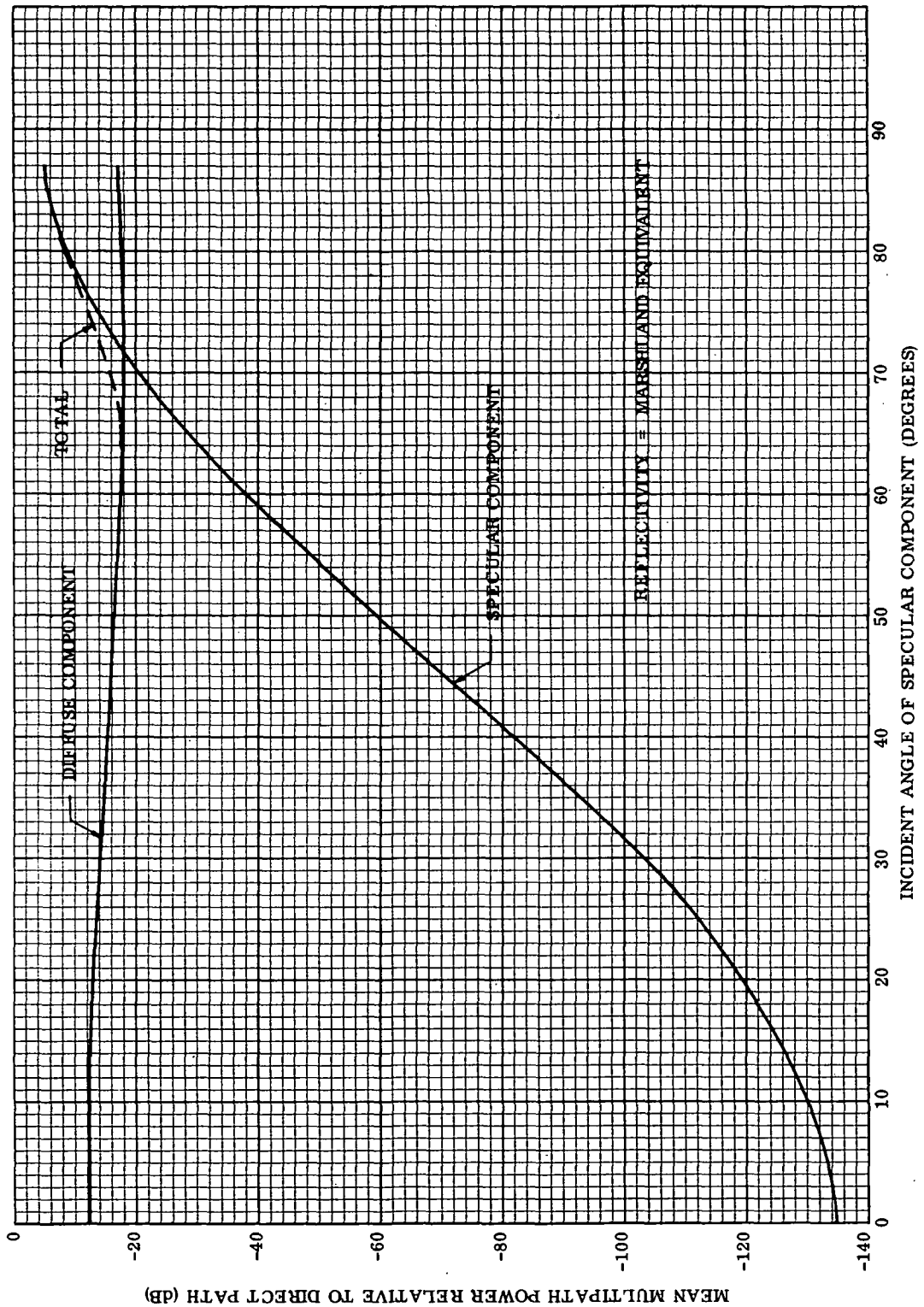

Figure 3-3. Relative Multipath Power for Aircraft/Synchronous Satellite Data Relay (σ = 1.0, T = 100)

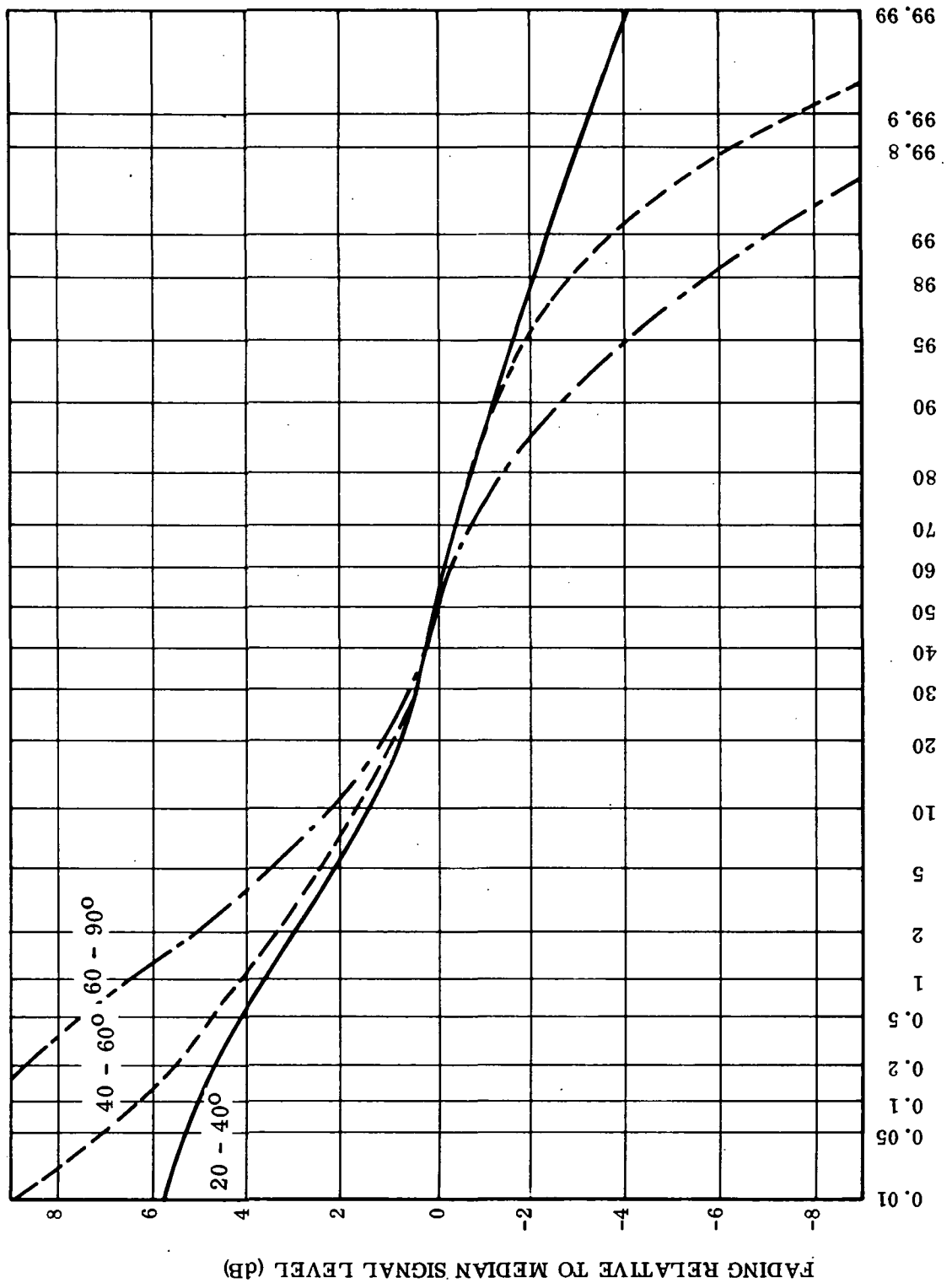

Figure 3-4. Probability Distribution of Signal Fading.
Source: Bergemann and Kucera[11]
Figure 15.

3.1 -- Continued.

For R_{10}/R_{90} = 2.5 dB, both models yield K = -16 dB. For R_{10}/R_{90} = 4.5 dB, both models yield approximately the same result, K = -12 dB.

Finally these values for K obtained from experimental data will be compared with the values for K obtained from the ESL model. In Figure 3-5, the results for total multipath from runs 1, 2, and 3 are plotted, along with the values of K obtained from the experimental data. The closest fit to the experimental data can be determined by calculating the median from the ESL model as shown in Table 3-1.

From Table 3-1, it can be seen that run number 3 (σ = 1.0, T = 100) gives the closest albeit poor overall fit to the experimental data. Thus, Figure 3-3 will be taken as the most probable representation of the actual situation. This figure provides the mean power in the multipath components relative to the direct path component, which can then be used to obtain the probability distributions of the resultant signal for various incidence angles. For incidence angles less than 60 degrees, the specular component is less than -40 dB and can be safely ignored. Therefore, the resultant signal is the sum of a constant direct path signal and a Rayleigh distributed diffuse component, which yields the Rice distribution. The resultant signal distributions for incidence angles less than 60 degrees are shown in Figure 3-6 for 10 degree increments in incidence angle.

For incidence angles greater than 60 degrees, the specular component cannot be ignored. Since the specular component generally fluctuates much more slowly than the diffuse component, the sum of the direct path signal and the specular component can be considered as a constant signal, so that interference with the diffuse component once again yields a Rice distributed resultant. For an incident angle of 70 degrees, Figure 3-3

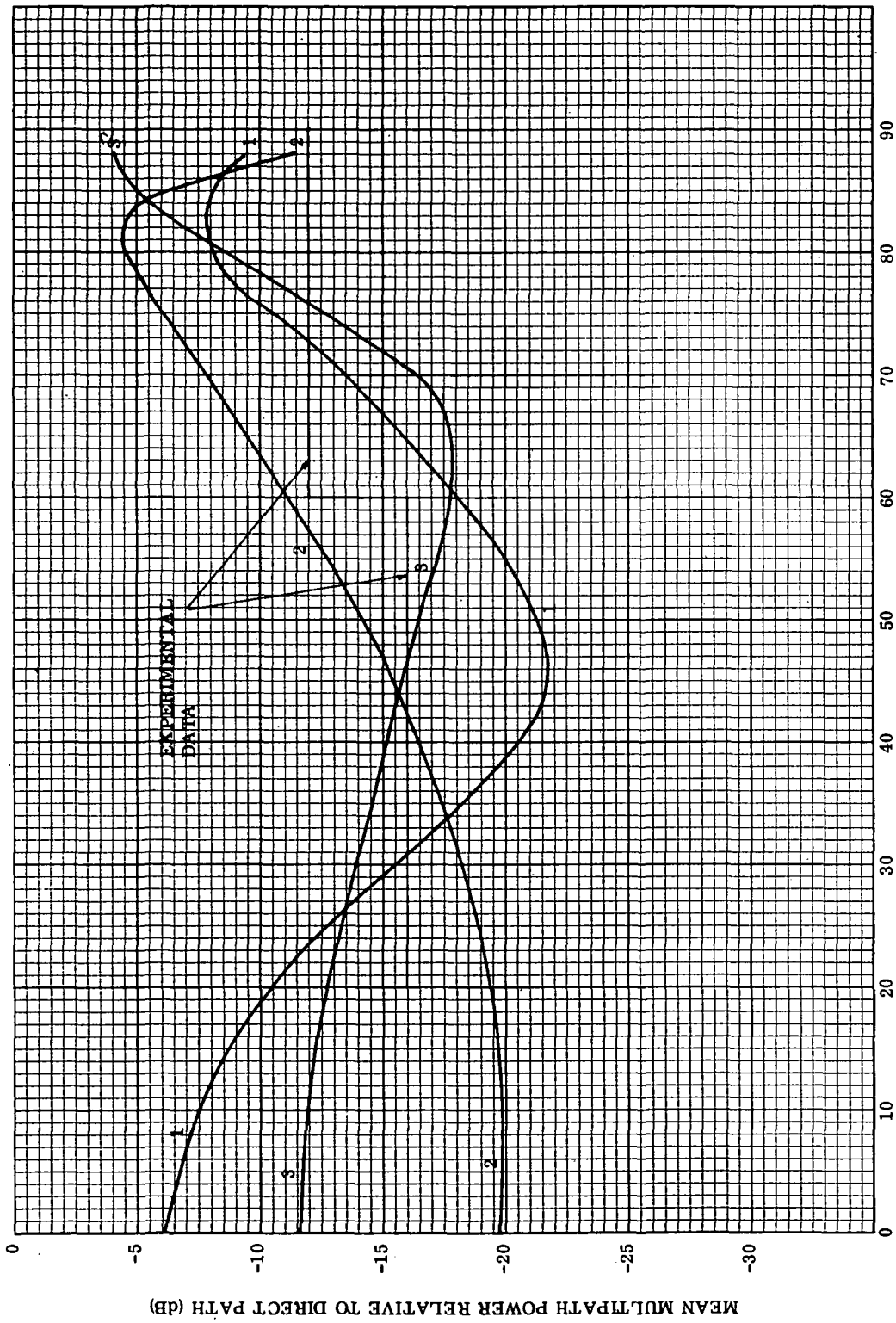

Figure 3-5. Total Multipath Power of Runs 1, 2 and 3 Compared With Experimental Data

Table 3-1. Median Power in Random Component Relative to Direct Path (dB)

Source	Incident Angle	
	20-60 (Degrees)	60-90 (Degrees)
Experimental Data (Bergemann and Kucera)[11]	-16.0	-12.0
Run No. 1 (σ = 1.0, T = 10)	-18.1	-11.4
Run No. 2 (σ = 0.5, T = 10)	-16.0	-7.6
Run No. 3 (σ = 1.0, T = 100)	-15.3	-11.8

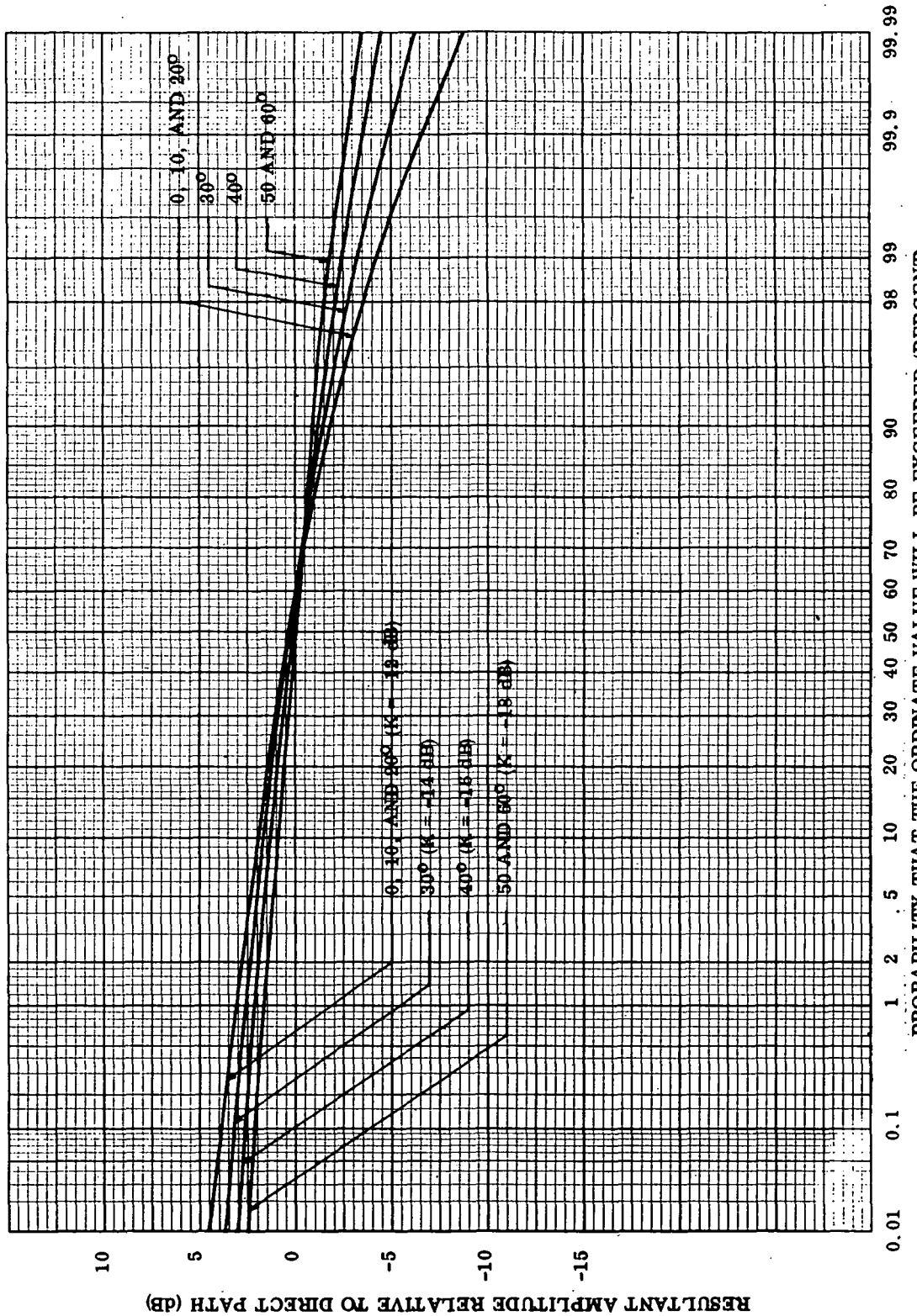

Figure 3-6. Resultant Signal Distributions for Aircraft/Synchronous Satellite (Incidence Angles 0 to 60 Degrees)

3.1 -- Continued.

indicates that the specular component is -20 dB and the diffuse component is -18 dB relative to the direct path. As shown in Figure 2-3 (the two-ray fading model), a -20 dB specular component causes about a 1 dB degradation in envelope level when distructive interference of direct and specular components occurs and about a 1 dB enhancement in envelope level when constructive interference occurs. A 1 dB degradation of the direct path envelope level means that the diffuse component is -17 dB relative to the constant signal component, instead of -18 dB. The probability distribution for the resultant signal relative to the direct path is thus obtained by shifting the Rice distribution for -17 dB downward by 1 dB (the amount of fading caused by the specular component) as shown in Figure 3-7. Similarly, a 1 dB enhancement in envelope level means that the diffuse component is -19 dB relative to the constant signal component instead of -18 dB. In this case, the probability distribution for the resultant signal relative to the direct path is obtained by shifting the Rice distribution for -19 dB upward by 1 dB (the amount of enhancement caused by the specular component) as shown in Figure 3-7. Thus, the two probability curves in Figure 3-7 form the upper and lower limits of fading distributions for an incidence angle of 70 degrees. Observe that even with distructive specular interference the fading is less than -3.5 dB for 99 percent of the time.

For an incidence angle of 80 degrees, the specular component is -8 dB and the diffuse component is -18 dB relative to the direct path, which from Figure 2-3 yields a 4 dB degradation for destructive specular interference and a +2.5 dB enhancement for constructive specular interference. Therefore, for destructive interference of direct and specular components, the diffuse component is -14 dB relative to the constant component and for constructive interference the diffuse component is -20.5 dB. The resulting

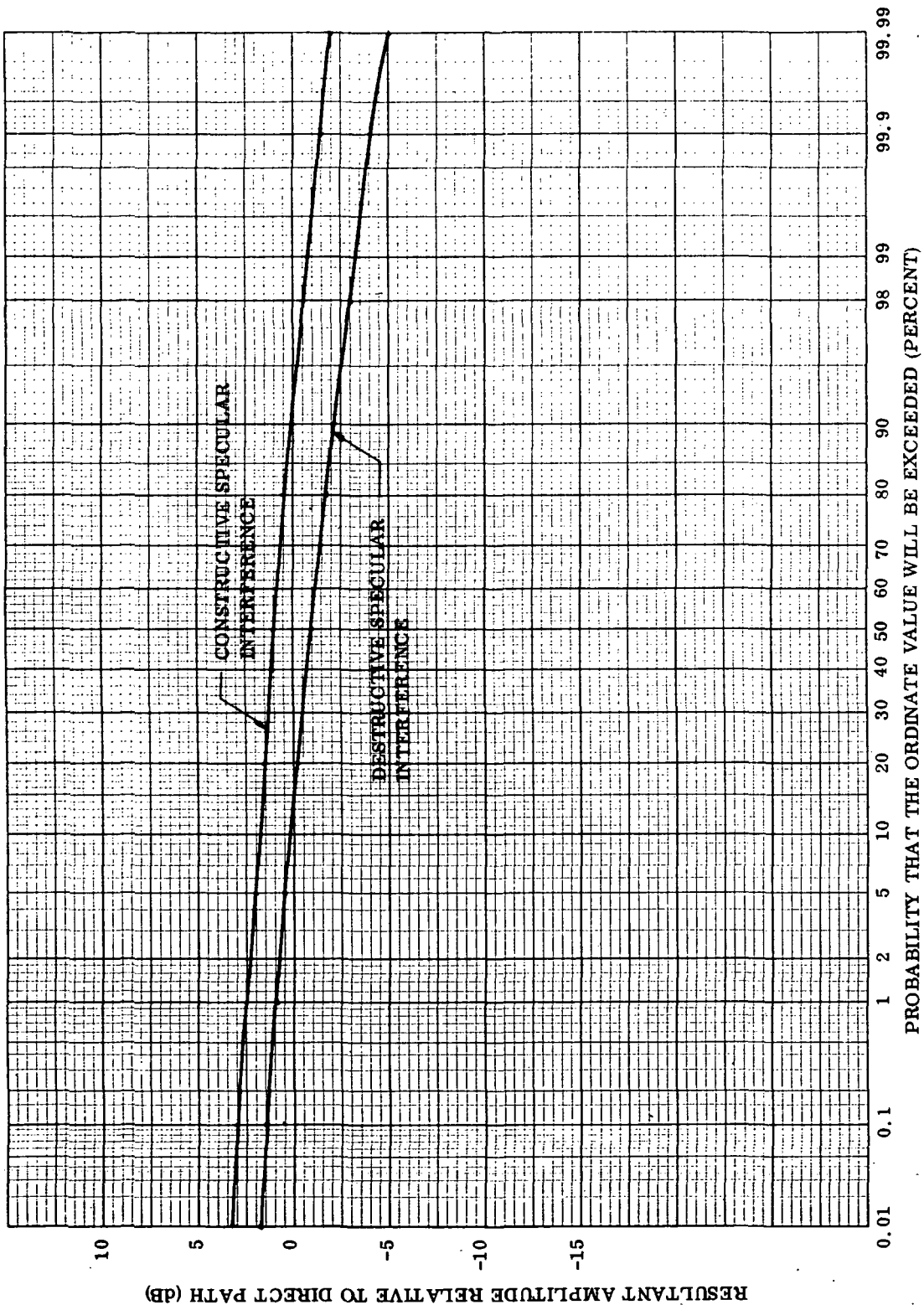

Figure 3-7. Resultant Signal Distributions for Aircraft/Synchronous Satellite (Incidence Angle = 70 Degrees)

3.1 -- Continued.

probability distributions for these values are shown in Figure 3-8. The curves of Figure 3-8 form the upper and lower limits of fading distributions for an incidence angle of 80 degrees. For destructive specular interference, the fading is less than -7.5 dB for 99 percent of the time.

In order to summarize the analysis of the aircraft/synchronous satellite data relay, Table 3-2 gives the resultant signal level (relative to the direct path) which is exceeded 99 percent of the time for various incidence angles.

3.2 Time and Frequency Dispersion.

Assuming an aircraft altitude of 10 kilometers, the range of possible multipath time delays is sketched in Figure 3-9. Since the specularly reflected multipath component is defined as the minimum time reflection path between the transmitter and receiver, the specular delay is given by the lower boundary of the shaded area. For the synchronous satellite directly overhead the specular delay is maximum and equals 67 microseconds and the diffuse delay ranges up to 1.2 milliseconds. The maximum delay of any diffuse component is 2.4 milliseconds.

The differential doppler shift between the direct path and the specularly reflected paths is less than 1 Hz for all angles of incidence at VHF.[12] However, the frequency spreading can be at least on order of magnitude higher and increases with angle[13] as shown in Figure 3-10. The maximum observed value is 50 Hz.

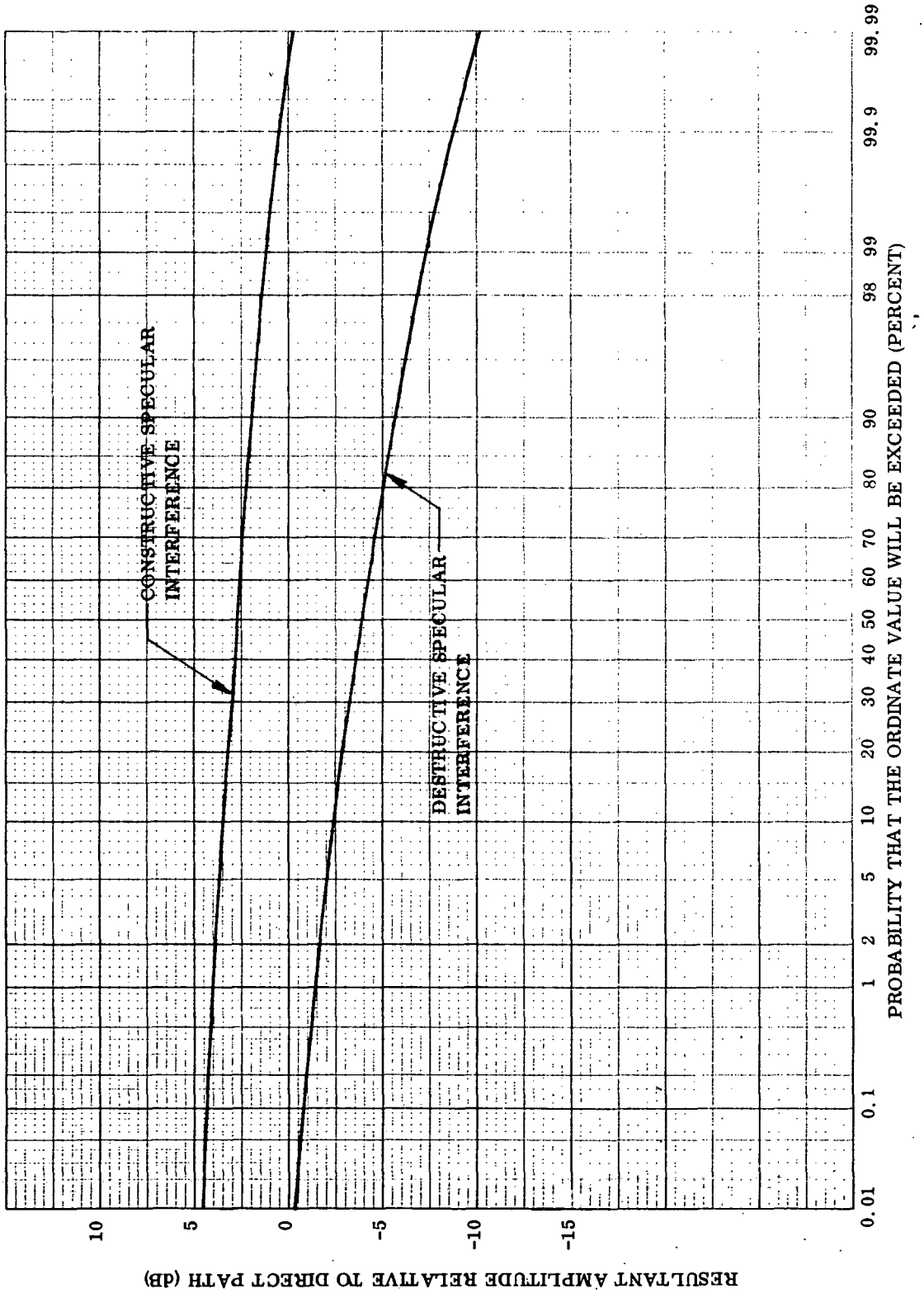

Figure 3-8. Resultant Signal Distribution for Aircraft/Synchronous Satellite (Incidence Angle = 80 Degrees)

Table 3-2. Summary of Aircraft/Synchronous Satellite Analysis (All dB Values are Relative to Direct Path Signal Level; Results Based on $\sigma = 1$, $T = 100$)

Incidence Angle (Degrees)	Resultant Signal Level Which is Exceeded 99 Percent of the Time (dB)
0, 10, 20	-4.5
30	-3.5
40	-2.5
50, 60	-2.0
70 Constructive Specular Interference	-1.0
70 Destructive Specular Interference	-3.5
80 Constructive Specular Interference	+1.0
80 Destructive Specular Interference	-7.5

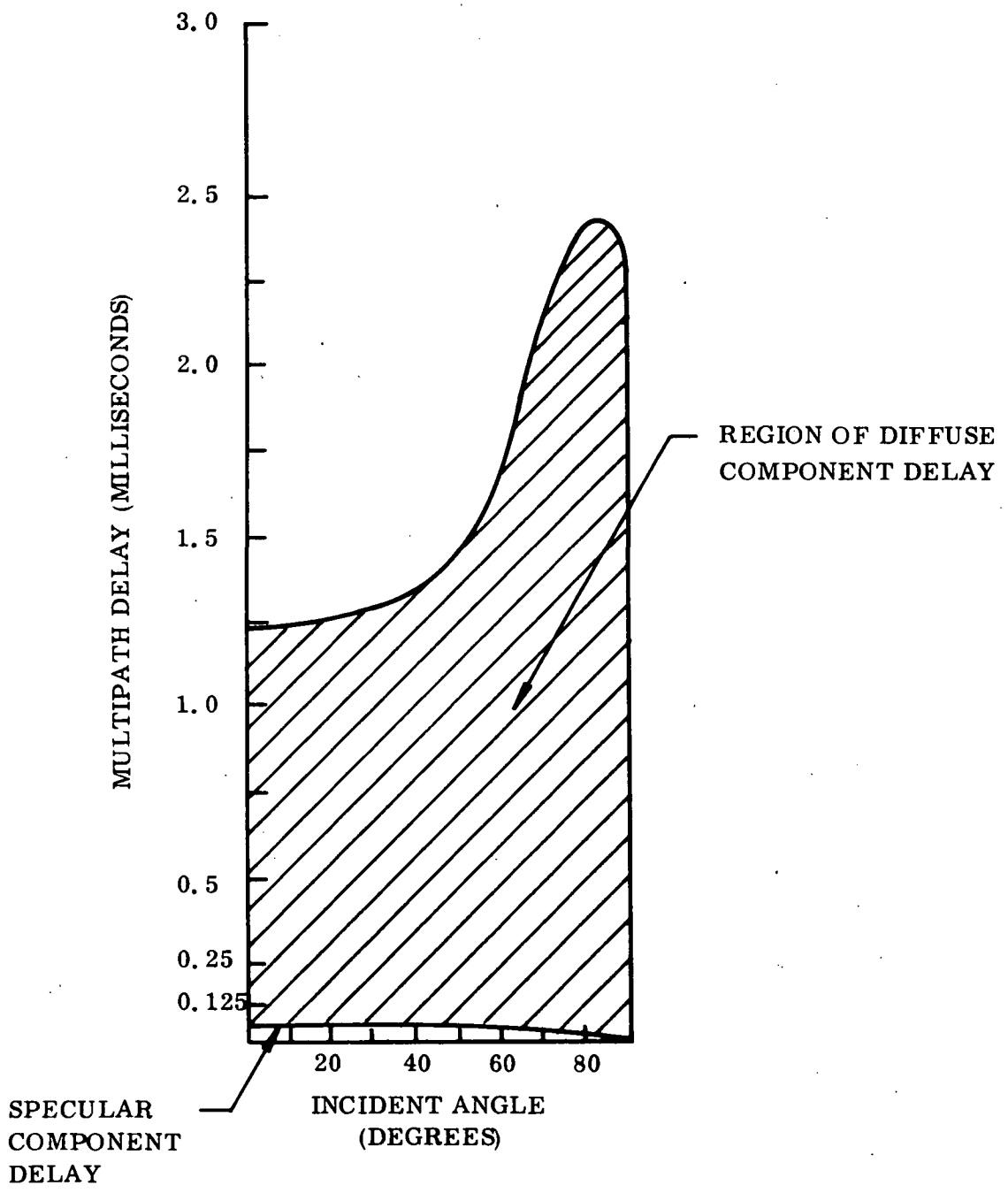

Figure 3-9. Range of Possible Multipath Delays for Aircraft/Synchronous Satellite Relay (Aircraft Altitude = 10 Kilometers).

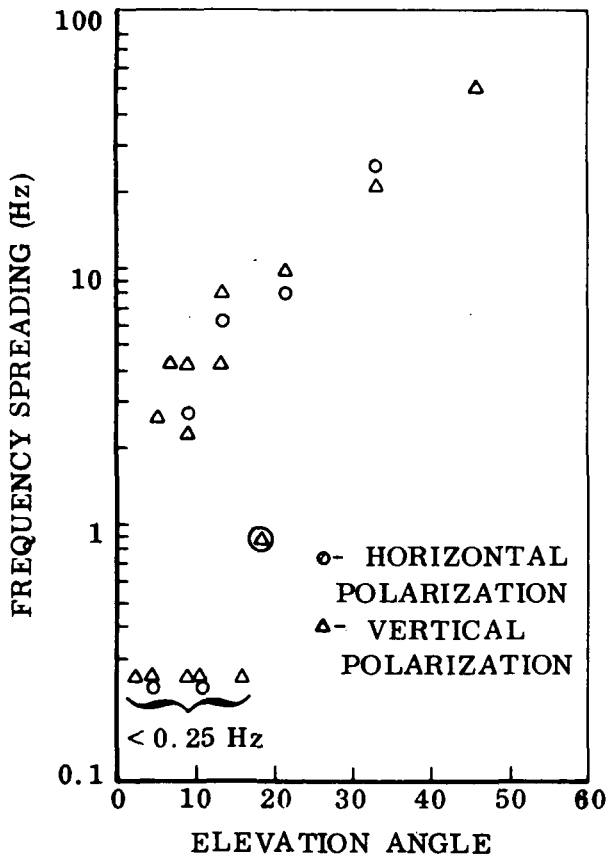

Figure 3-10. Frequency Spreading for Aircraft/Synchronous Satellite Relay: Source Jordan[13]

3.3 Channel Transfer Function.

For the moment assume that there are no time variations. The channel transfer function is then given by Equation (2-3), i.e.,

$$H(f) = 1 + \sum_{i=0}^{n} k_i \exp[-j2\pi f\tau_i]$$

An example of the use of this transfer function when the multipath consists of specular reflection only with a magnitude of -6 dB relative to the direct path was shown previously in Figure 2-10, using a 130 MHz carrier frequency and a differential time delay of 65 microseconds. As predicted, the distance between magnitude peaks (or nulls) is given by 1/65 microseconds = 15.4 kHz. Also, note that phase shifts of up to ± 60 degrees can occur.

If, in addition to specular reflection, diffuse scattering occurs, then a Rayleigh vector must be simulated to represent the diffuse component. As described in Section 2.2, a Rayleigh vector can easily be generated from the sum of six or more sine waves with equal amplitudes and uniformly distributed phases. Furthermore, since the individual components are independent of each other, the average power of the resultant equals the sum of the average power of the components. Therefore, a Rayleigh vector with average power P can be generated from the sum of n vectors of equal amplitudes and uniformly distributed phases such that

$$P = nP_o$$

3.3 -- Continued.

where P_o is the power of a single component vector. For a formal proof of this relationship, see Beckmann and Spizzichino.[3]

The magnitudes of the multipath components estimated by the ESL model for the aircraft/synchronous satellite case (Figure 3-3) are shown in Table 3-3. Typical transfer functions at a point in time for the values in Table 3-3 are shown in Figures 3-11, 3-12 and 3-13. The amount of distortion described by these three situations is fairly similar, with the maximum and minimum magnitudes (relative to 1.0) given by (1.2, 0.8), (1.25, 0.8), and (1.55, 0.7) for 0-60, 70, and 80 degrees respectively.

The results shown in Figures 3-11, 3-12, and 3-13 may be considered typical at any instant of time. However, the positions of the peaks and nulls vary in time at a rate given by the doppler spread. Thus, a distinctively different pattern can be anticipated approximately every tenth of a second, and even as often as every 0.02 seconds.

We see that significant distortion of the transfer function can occur due to multipath. The impact on the performance of communication systems is analyzed in Sections 6 and 7.

Table 3-3. Mean Power of Multipath Components of Figure 3-3 (Aircraft/Synchronous Satellite)

Incidence Angle (Degrees)	Diffuse	Specular
0-60	-15 dB	<-40 dB
70	-18 dB	-20 dB
80	-18 dB	-9 dB

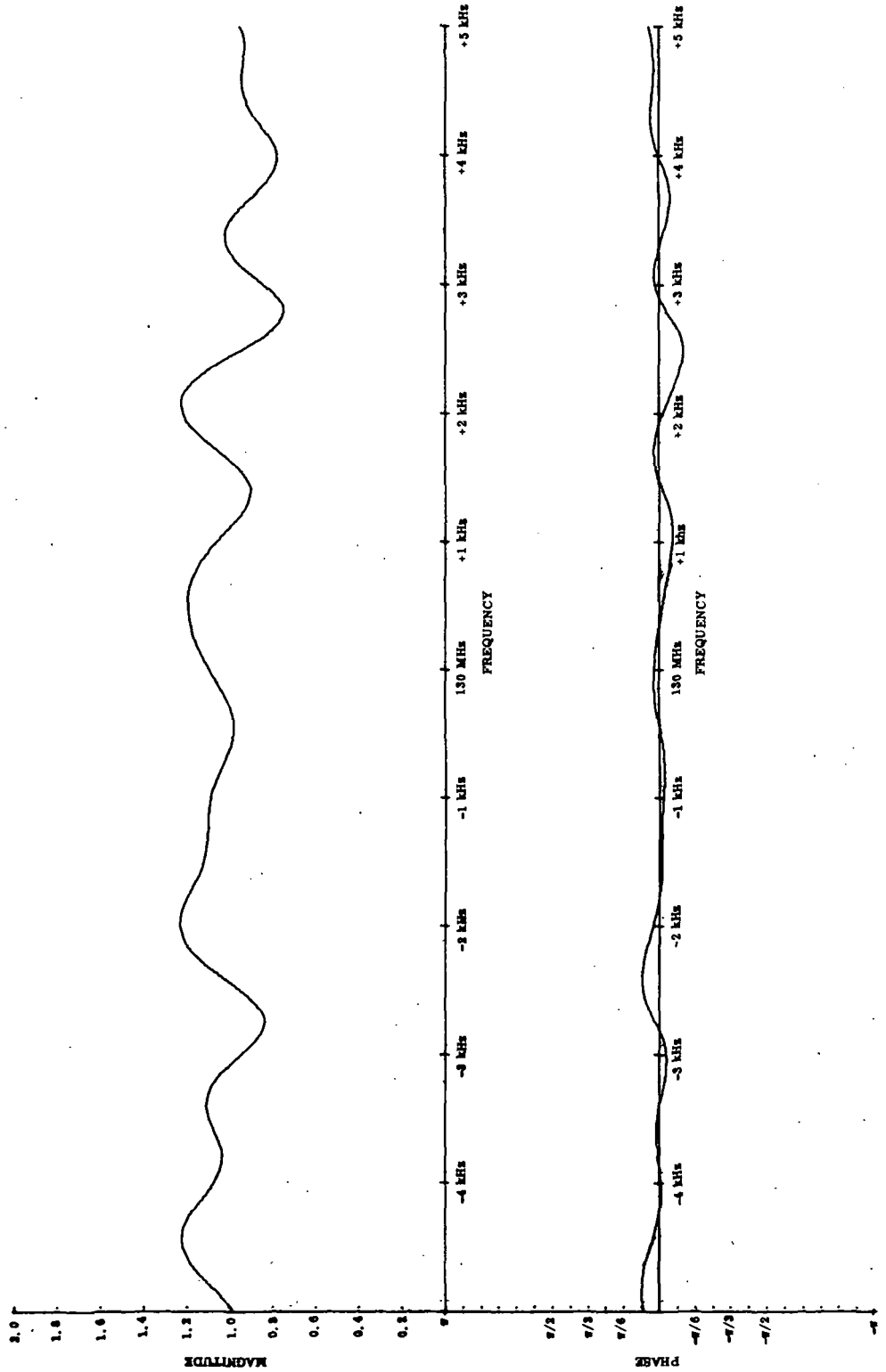

Figure 3-11. Typical Transfer Function for Aircraft/Synchronous Satellite Relay for Incidence Angles (0 thru 60 Degrees)

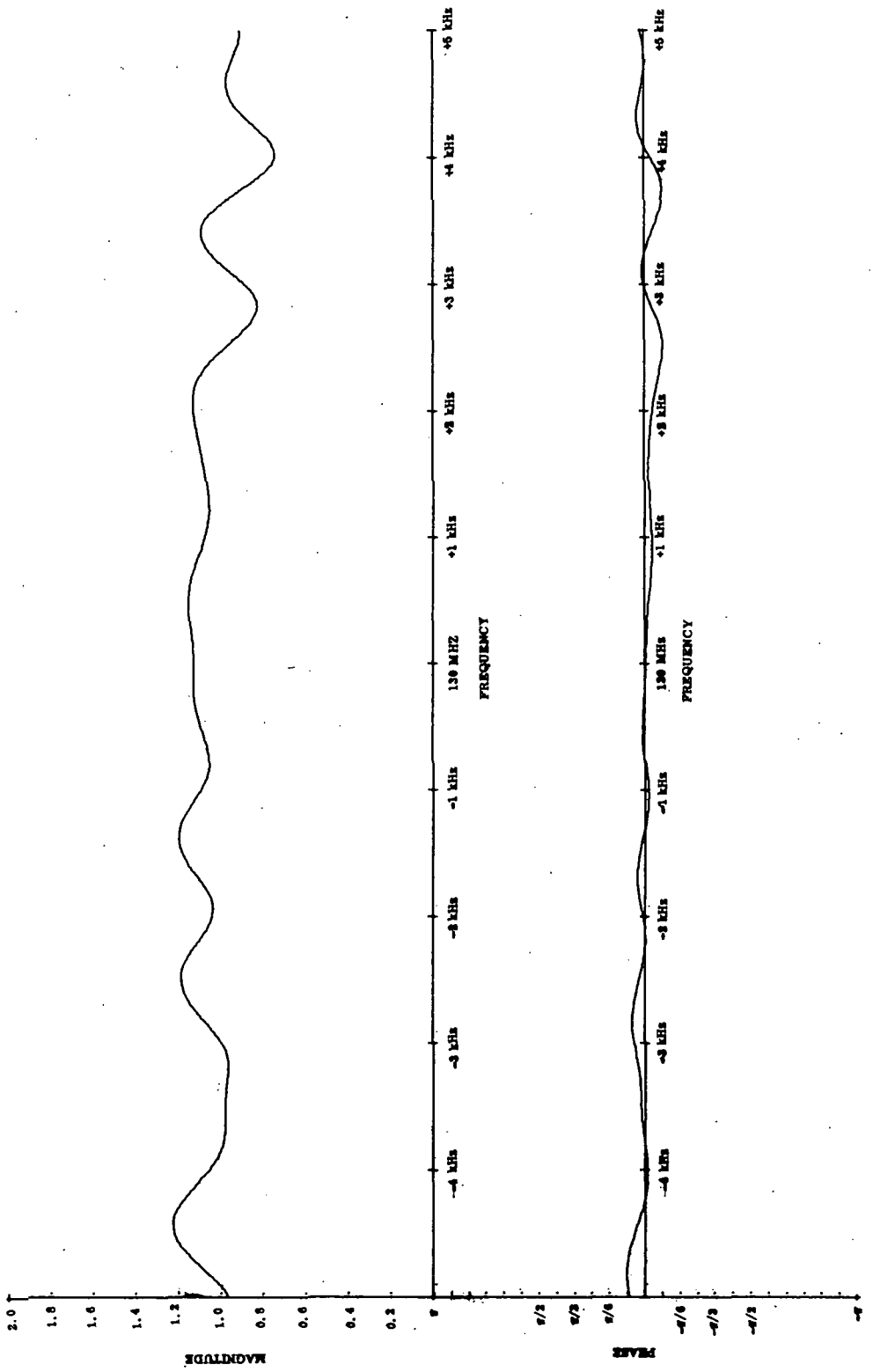

Figure 3-12. Typical Transfer Function forAircraft/Synchronous Satellite Relay for Incidence Angle = 70 Degrees

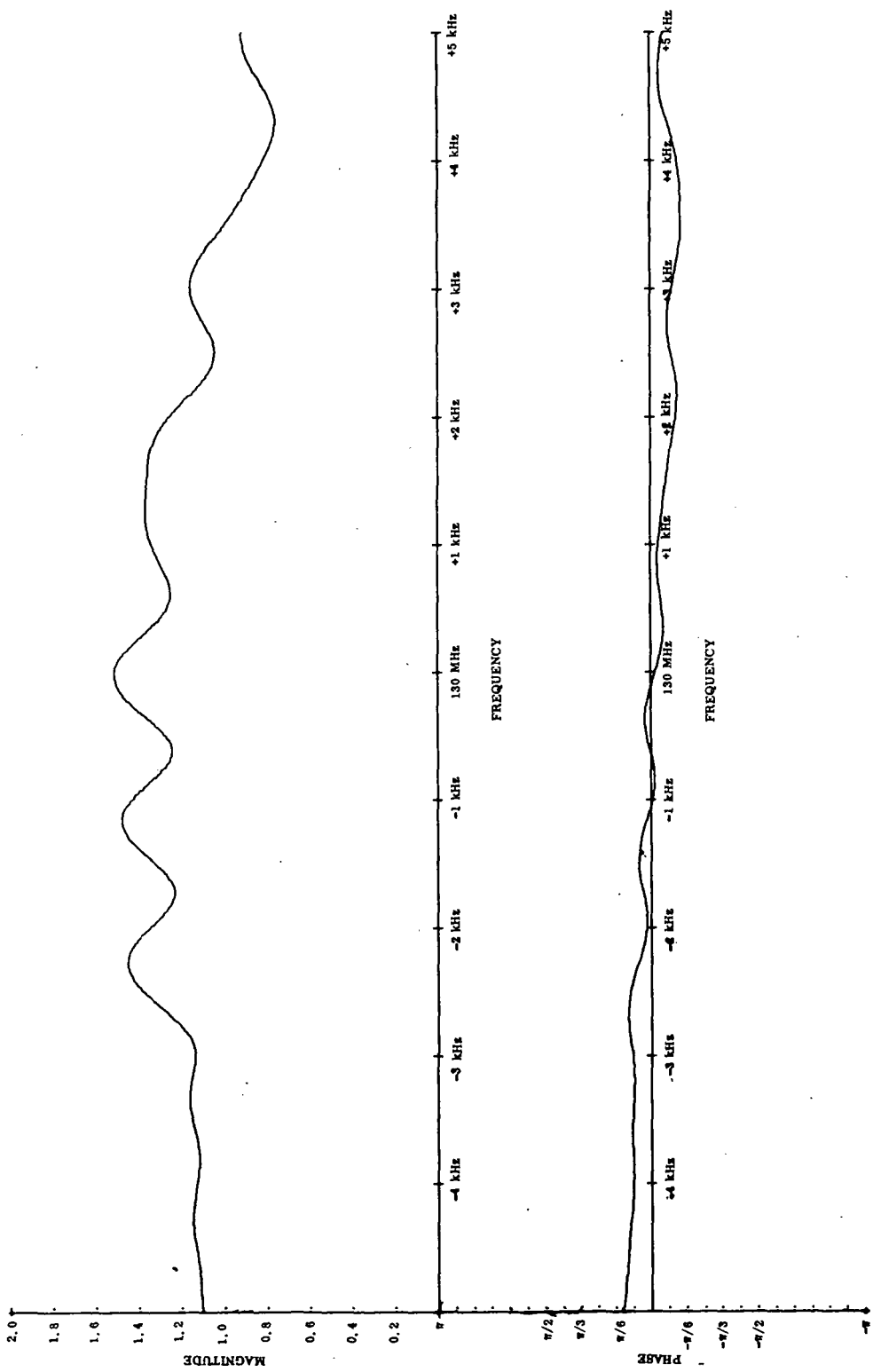

Figure 3-13. Typical Transfer Function for Aircraft/Synchronous Satellite Relay for Incidence Angle = 80 Degrees

4. WEATHER SATELLITE/SYNCHRONOUS SATELLITE RELAY.

4.1 Expected Magnitude of Multipath. The ESL multipath prediction model was applied to the weather satellite/synchronous satellite case with the following parameters:

Signal Frequency = 136 MHz

Weather Satellite Altitude = 1100 kilometers

Surface Reflectivity = Marshland Equivalent

	Surface Roughness (Meters)	Correlation Length (Meters)
Run No. 1	1.0	10.0
Run No. 2	0.5	10.0
Run No. 3	1.0	100.0

Run No. 1 can be viewed as the nominal situation and has the greatest amount of surface irregularity. Run No. 2 has reduced surface roughness compared with Run No. 1 and Run No. 3 has increased correlation length compared with Run No. 1. The results of Runs 1, 2, and 3 are shown in Figures 4-1, 4-2, and 4-3. respectively. Several general observations can be made from these figures: 1) the specular component is very sensitive to surface roughness but not to correlation length, 2) for Runs No. 1 and No. 3 with $\sigma = 1.0$, the specular component is much less than the diffuse component for incident angles less than 60 degrees, and 3) for Run No. 3 the diffuse component is nearly constant up to 70 degrees.

Run No. 3 will be taken as the best representation of the true situation, for two reasons: 1) experimental data indicates that the diffuse component is not a function of incidence angle, and the diffuse component of Run No. 3 is nearly constant for a wide range of

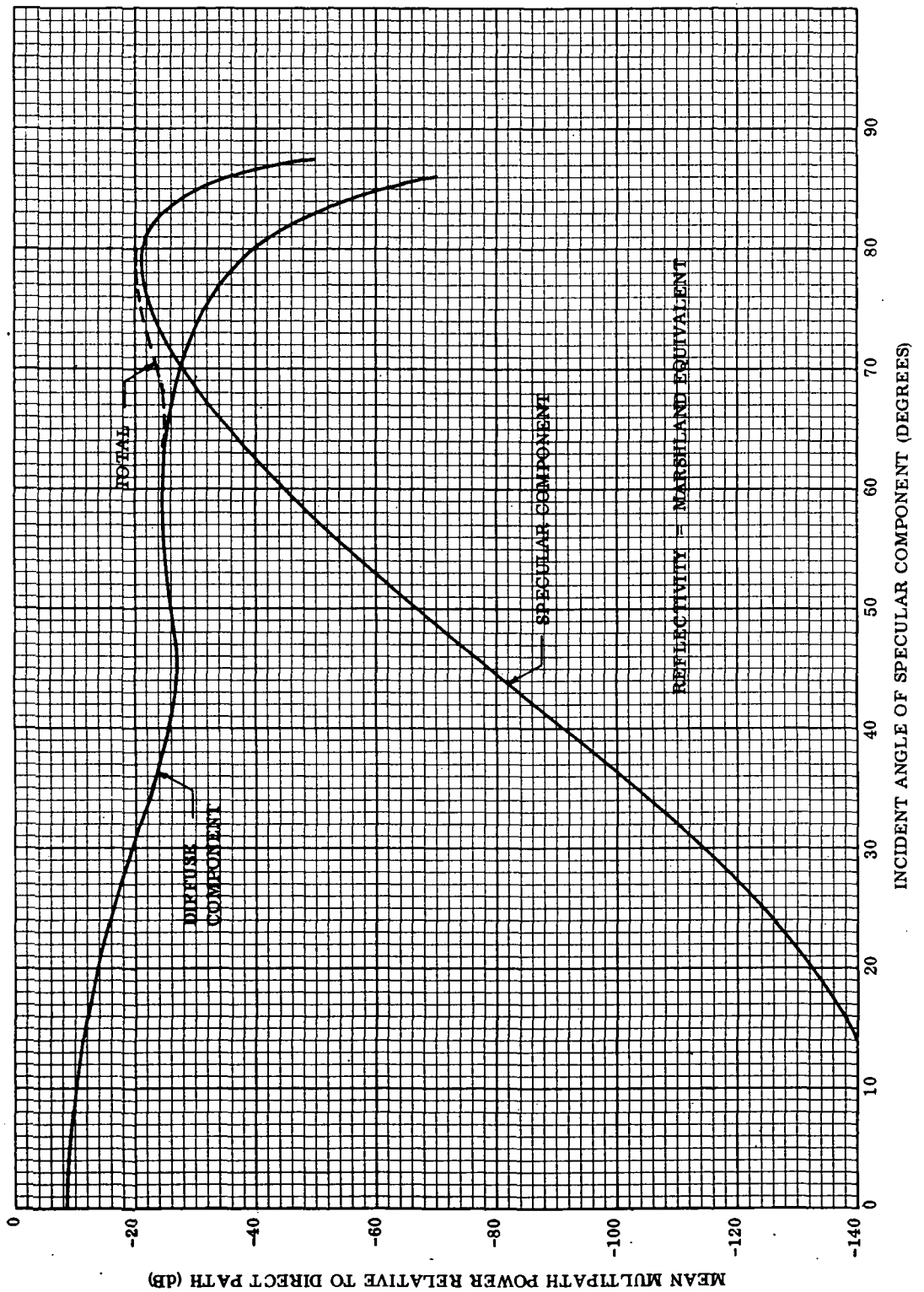

Figure 4-1. Relative Multipath Power for Weather Satellite/Synchronous Satellite Data Relay (σ = 1.0, T = 10.0)

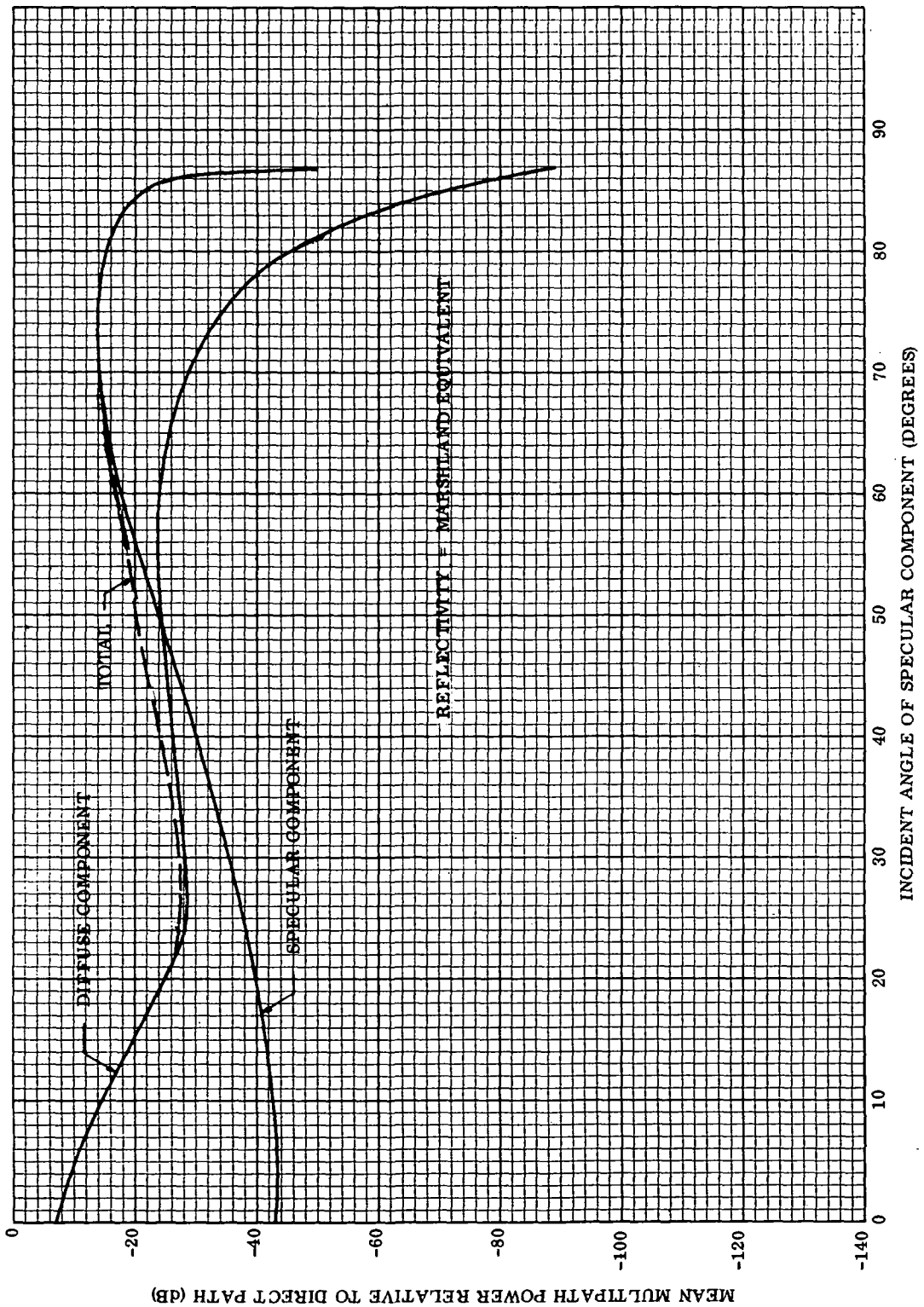

Figure 4-2. Relative Multipath Power for Weather Satellite/Synchronous Satellite Data Relay ($\sigma = 0.5$, $T = 10.0$)

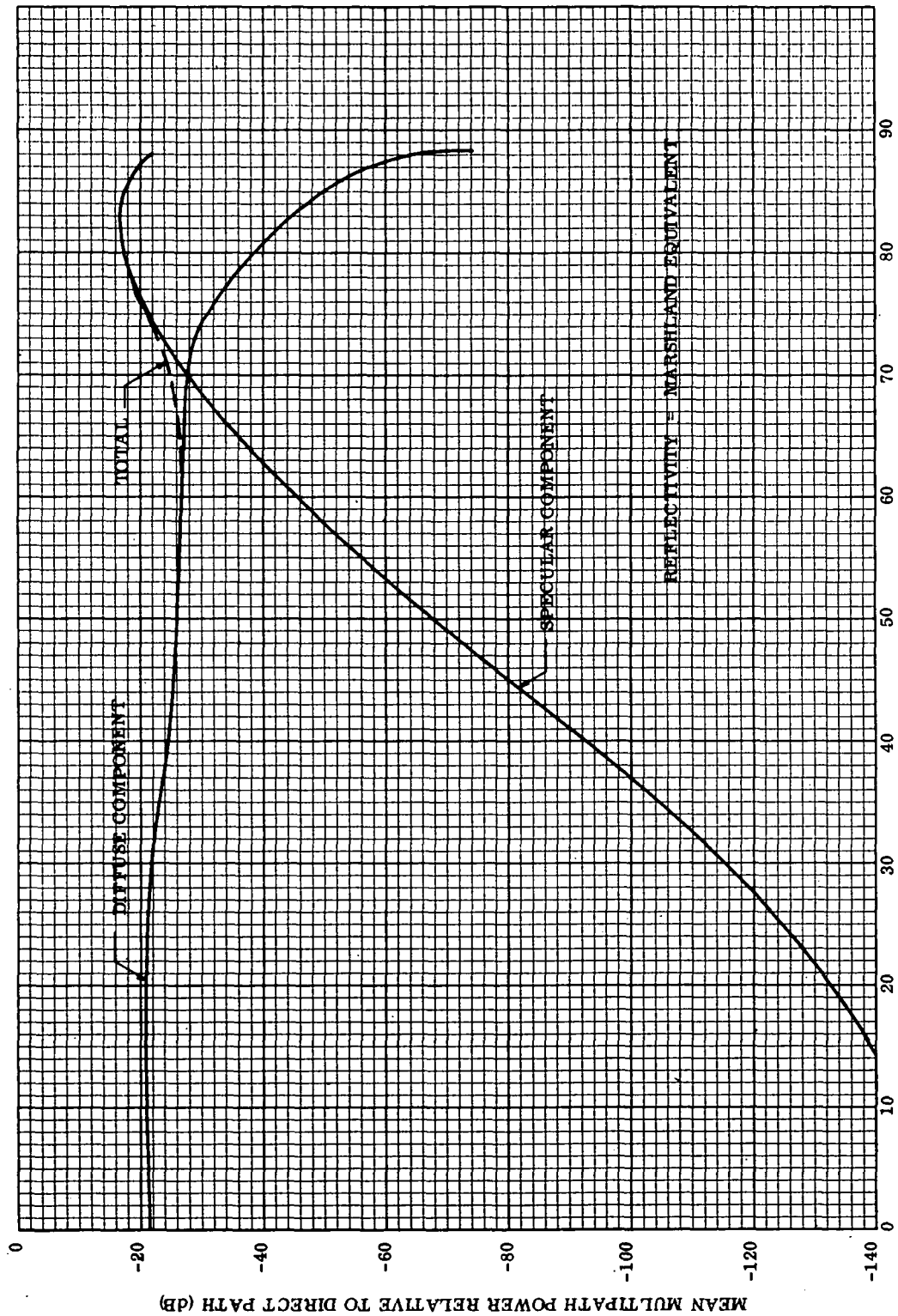

Figure 4-3. Relative Multipath Power for Weather Satellite/Synchronous Satellite Data Relay (σ = 1.0, T = 100.0)

4.1. -- Continued.

incidence angles and 2) the surface roughness and correlation length of Run No. 3 are the same as determined previously from experimental aircraft/synchronous satellite data. Since these parameters are a function only of the earth's surface characteristics, they should be valid for any satellite relay geometry.

The expected fading due to multipath will be obtained by applying the same procedure as used in Section 3 to the results of Figure 4-3. For incidence angles less than 60 degrees, the specular component is less than -40 dB and can be safely ignored. Therefore, the fading of the resultant signal is caused only by the diffuse component, which yields a Rice distribution. The resultant signal distributions for incidence angles less than 60 degrees are shown in Figure 4-4.

For incidence angles greater than 60 degrees, the specular component is taken into account as in Section 3 by combining the specular component with the direct path signal to obtain the constant signal which is interfered with by the diffuse component to yield a Rice-distributed resultant. For an incidence angle of 70 degrees, the specular component is -28 dB relative to the direct path. According to the two-ray fading model of Figure 2-3, a -28 dB specular component causes negligable fading in envelope level (a fraction of a dB). Therefore, the principal cause of fading will be the diffuse component, which is also at -28 dB. The Rice distribution for this value is also shown in Figure 4-4.

For an incidence angle of 80 degrees, the specular component is -18 dB and the diffuse component is -38 dB. Thus, in this case, the fading due to the diffuse component is negligable so that the fading can be represented solely by the two-ray fading model, with the result as shown in Figure 4-5.

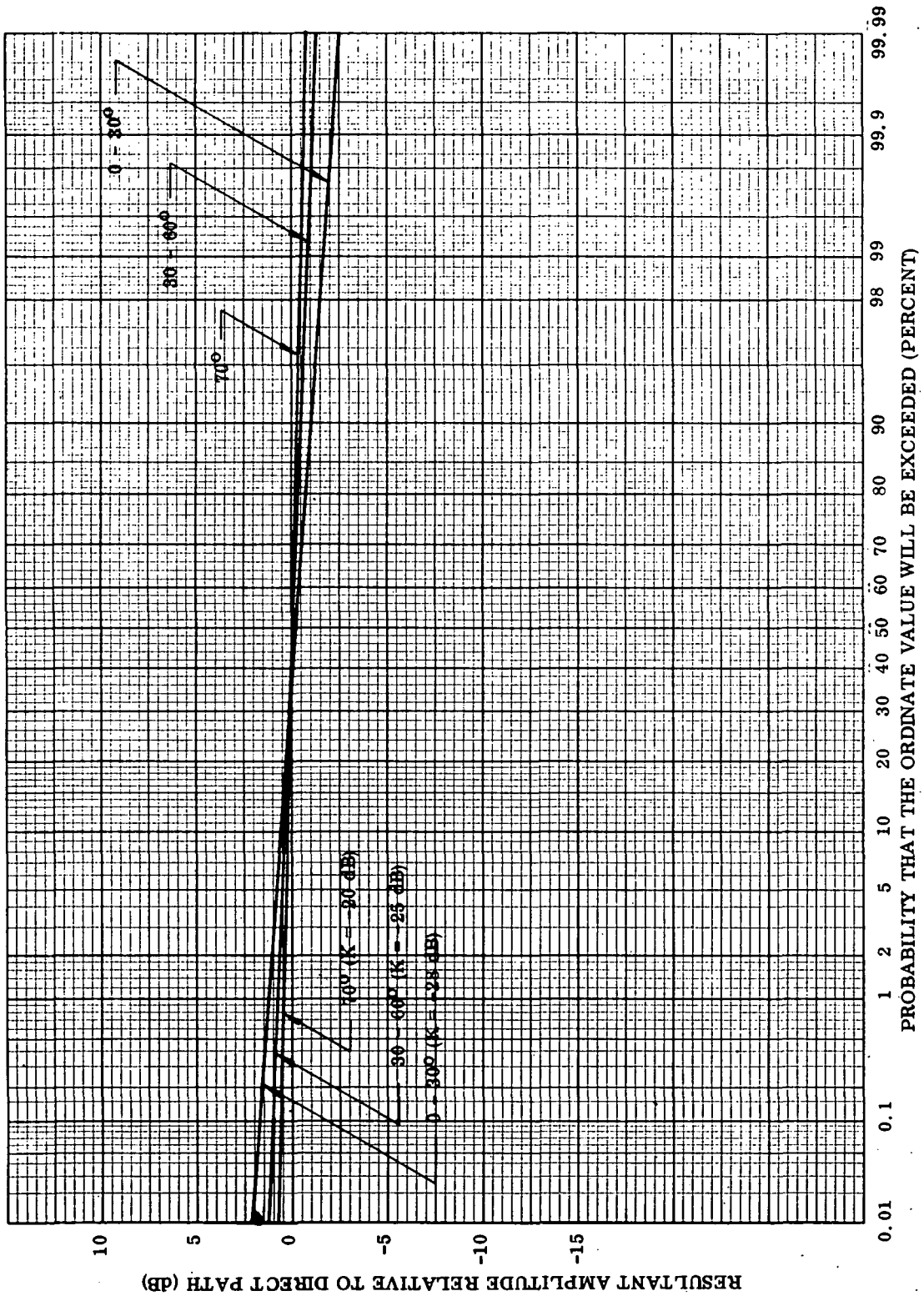

Figure 4-4. Resultant Signal Distributions for Weather Satellite/Synchronous Satellite (Incidence Angle = 0 Through 70 Degrees)

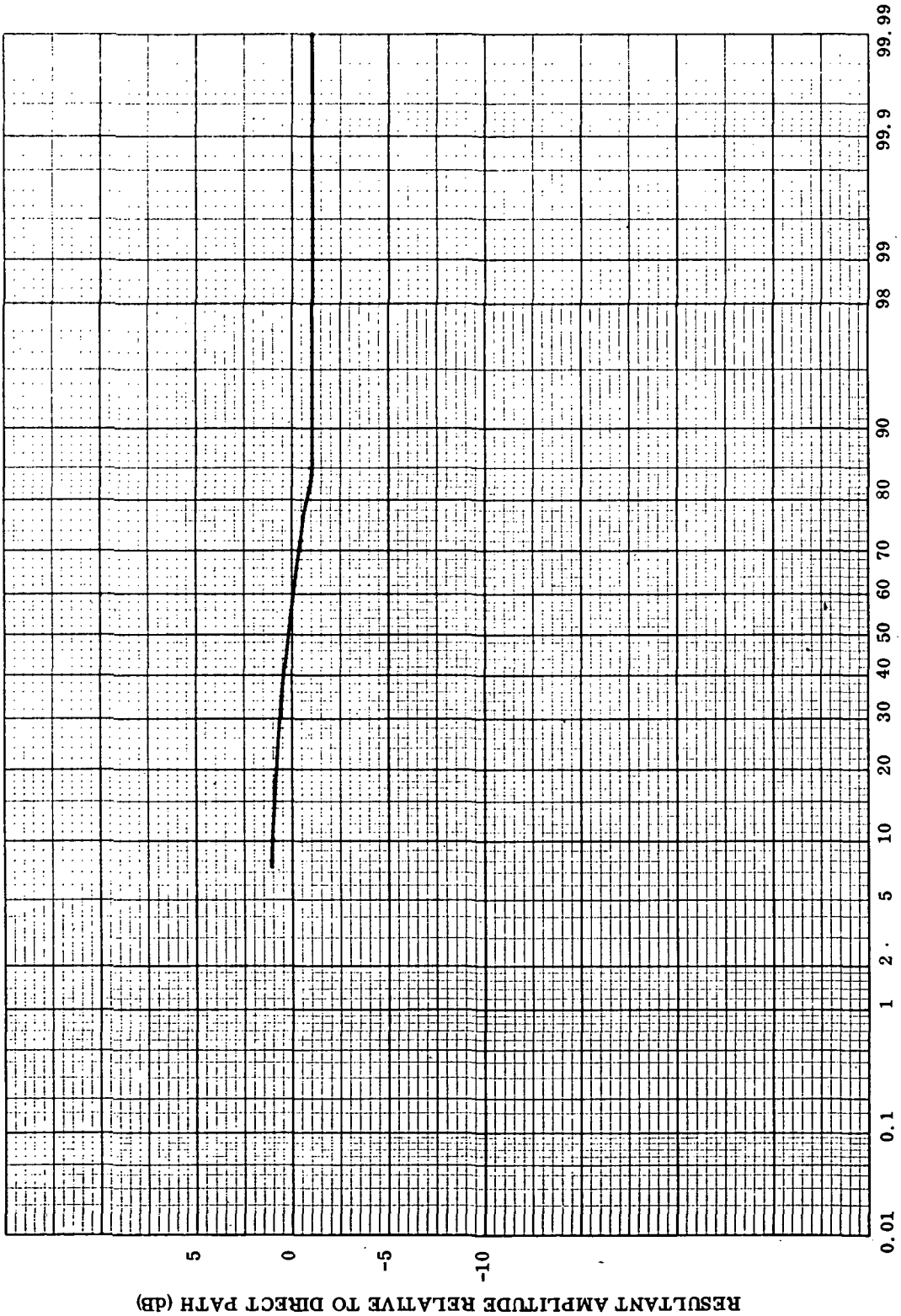

Figure 4-5. Resultant Signal Distribution for Weather Satellite/Synchronous Satellite (Incidence Angle = 80 Degrees)

4.1 -- Continued.

The results of this analysis can be summarized in Table 4-1, which gives the resultant signal level (relative to the direct path) which is exceeded 99 percent of the time for various incidence angles. In conclusion, it can be seen that the expected fading due to multipath for a weather satellite (at 1100 kilometers orbit)/synchronous satellite relay is less than 1 dB for 99 percent of the time for all angles of incidence.

4.2 Time and Frequency Dispersion.

Assuming the weather satellite has an altitude of 1100 kilometers, the range of possible multipath time delays is sketched in Figure 4-6. The specular component is given by the lower boundary of the shaded area. For the satellite directly overhead, the

Table 4-1. Summary of Weather Satellite/Synchronous Satellite Analysis (All dB Values are Relative to Direct Path Signal Level)

Incidence Angle (Degrees)	Resultant Signal Level Which is Exceeded 99 Percent of the Time (dB)
0 - 30	-1.0
30 - 60	-0.8
70	-0.5
80	-1.0

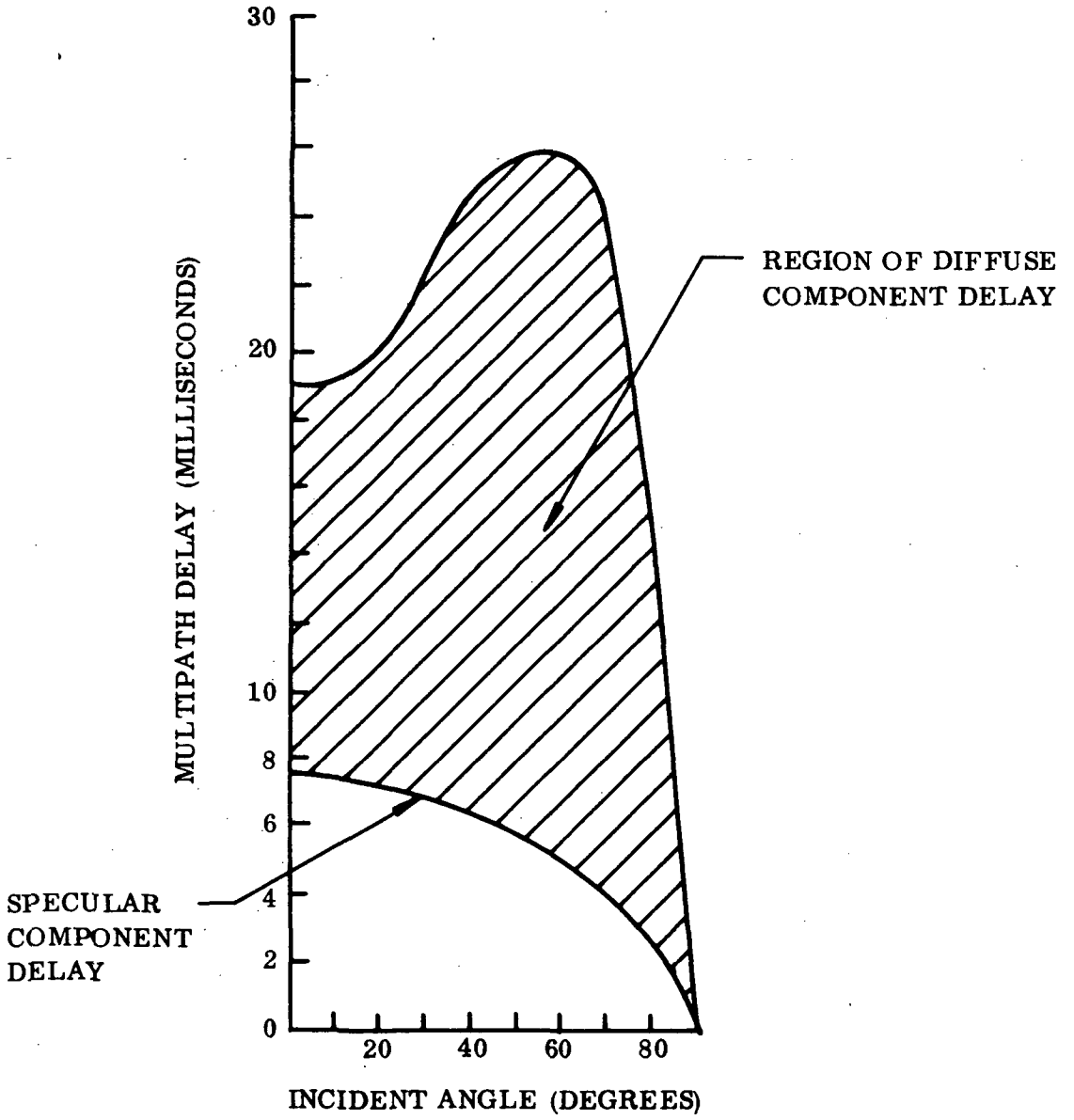

Figure 4-6. Range of Possible Multipath Delays for Weather Satellite/ Synchronous Satellite Relay

4.2 -- Continued.

specular delay is maximum and equals 7.3 milliseconds and the diffuse component delay ranges up to 19.0 milliseconds. The maximum delay of any diffuse component is 26.0 milliseconds.

The differential doppler shift between direct and specularly reflected paths is a function of incidence angle[14] and is shown in Figure 4-7. Observe that the differential doppler is always less than 800 Hz (for the specular component). The diffusely scattered signal produces a spread in doppler frequencies due to the large area of the scattering surface which is mutually visible from both transmitter and receiver. Estimates of this bandwidth have been derived by Durrani and Staras[15] and are shown in Figure 4-8.

4.3 Channel Transfer Function.

As was done in Section 3.3 for the aircraft/synchronous satellite case, typical channel transfer functions can be calculated for all desired incidence angles. The magnitudes of the multipath components estimated by the ESL model in Figure 4-3 are given in Table 4-2. Typical transfer functions at a point in time for the values in Table 4-2 are shown in Figure 4-9, 4-10, and 4-11, respectively.

All three of the typical transfer functions have a maximum deviation of ±10 percent in magnitude and ±7.5 degrees in phase from the direct path signal. When these results are compared with the aircraft/synchronous satellite results of Section 3.3, a significant decrease in distortion is apparent. The transfer functions will change significantly over a period of 1 millisecond. The impact of these transfer function distortions on communication system performance is detailed in Sections 6 and 7 following a summary of electromagnetic interference.

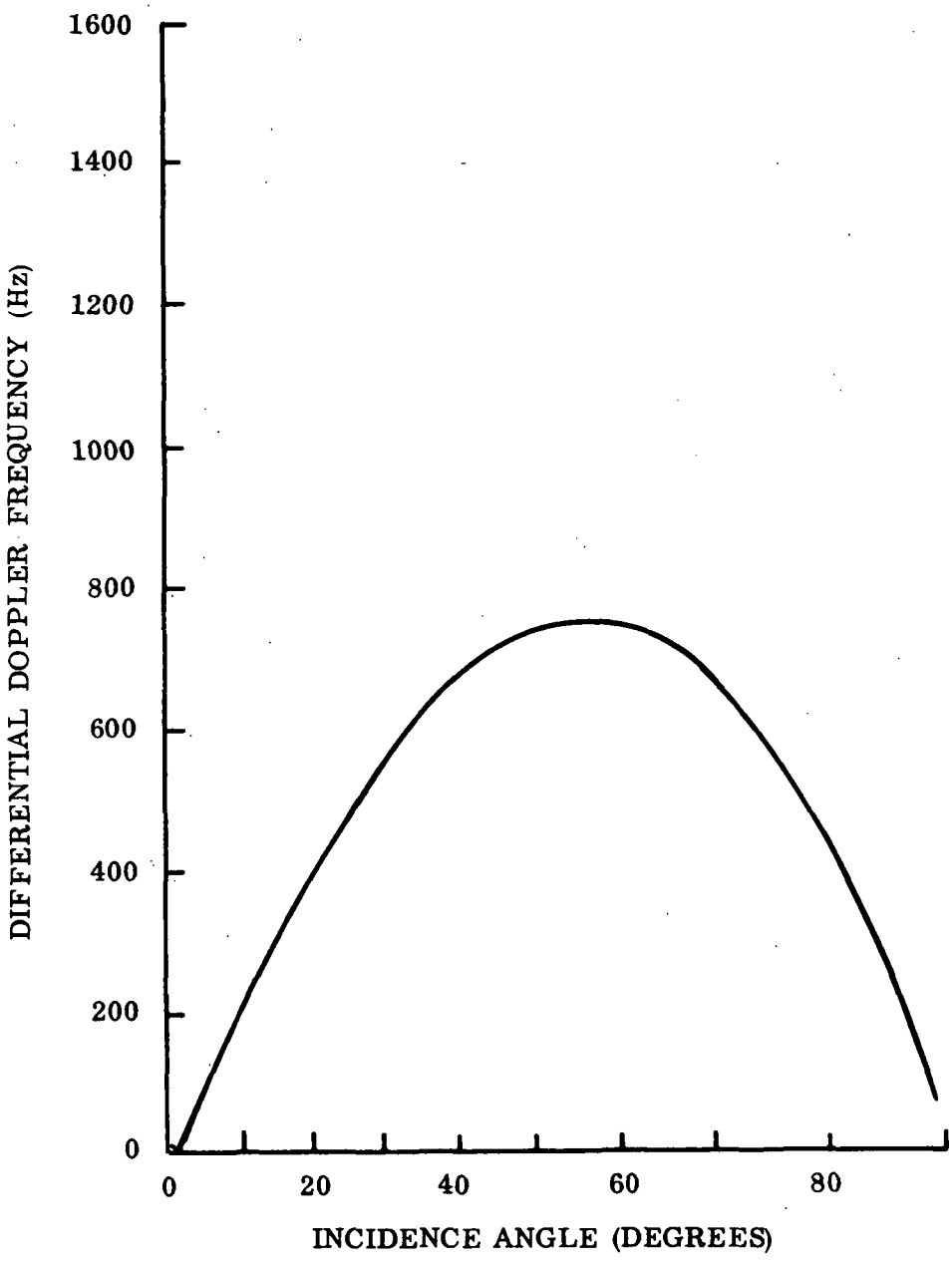

Figure 4-7. Difference in Doppler Frequencies Between Direct and Reflected Paths for 136 MHz Carrier

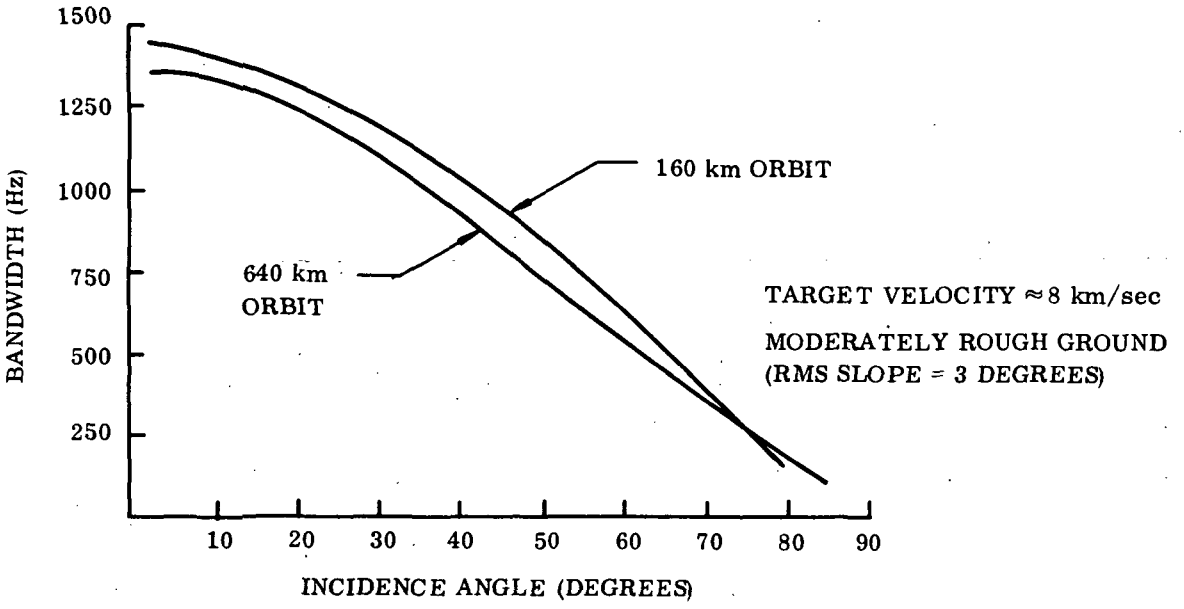

(a) Case I. Target Orbit in the Plane of the Target, Satellite, and Earth Center

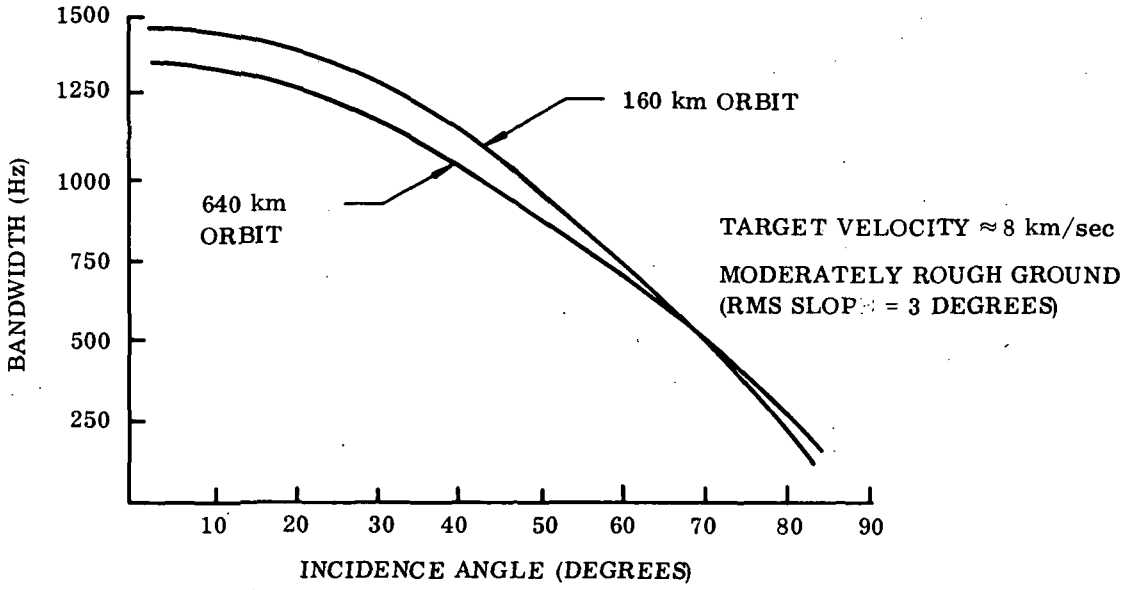

(b) Case II. Target Orbit Perpendicular to the Plane of the Target, Satellite, and Earth Center

Figure 4-8. Bandwidth of Scattered Signal for 136 MHz Carrier Frequency
Source: Durrani and Staras.[15]

Table 4-2. Mean Power of Multipath Components of Figure 4-3 (Weather Satellite/Synchronous Satellite Relay)

Incidence Angle (Degrees)	Diffuse (dB)	Specular (dB)
0 - 60	-22	<-40
70	-28	-28
80	-38	-18

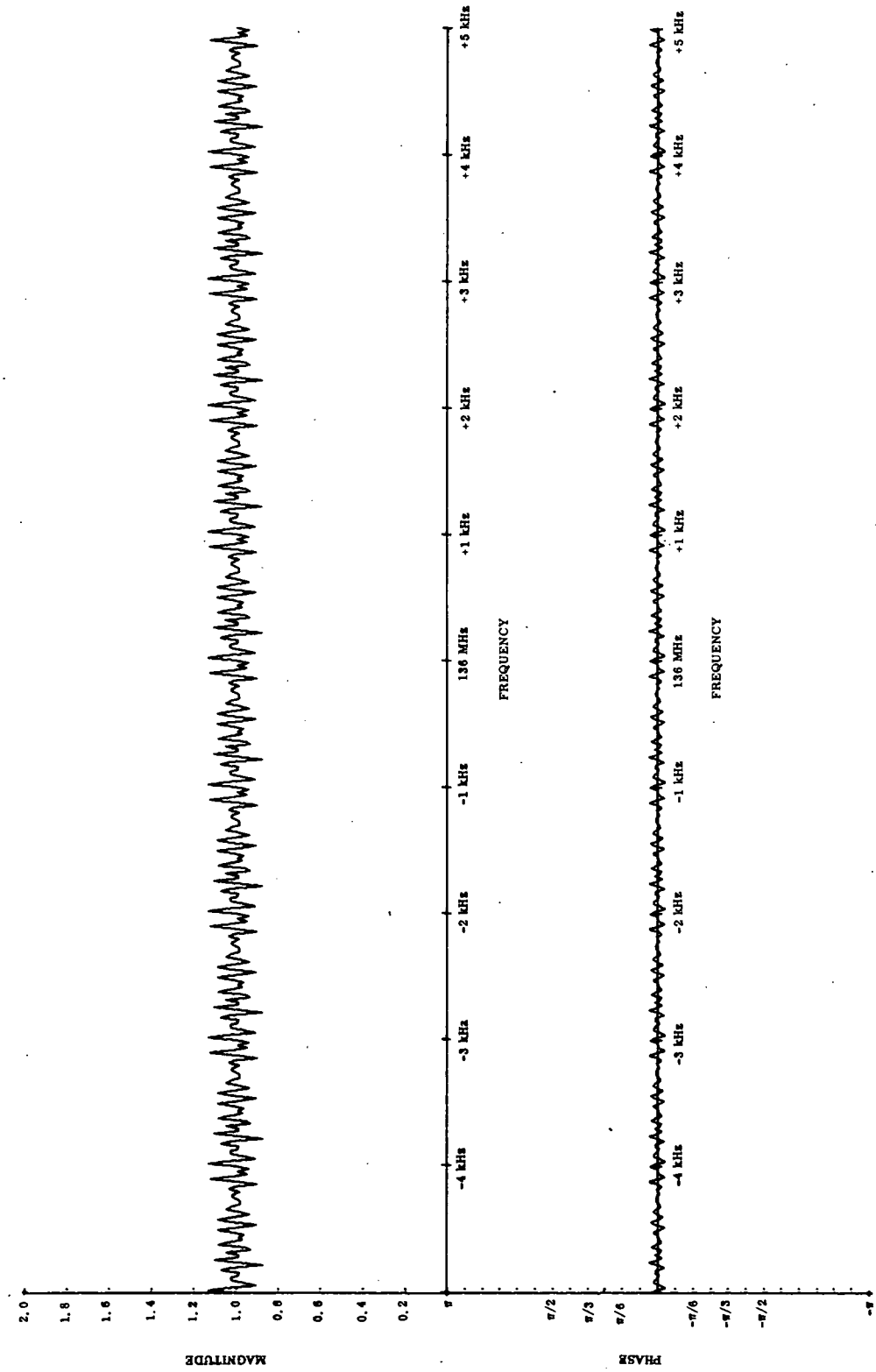

Figure 4-9. Typical Multipath Channel Transfer Function for Weather Satellite/ Synchronous Satellite Relay (Incidence Angles 0 Through 60 Degrees)

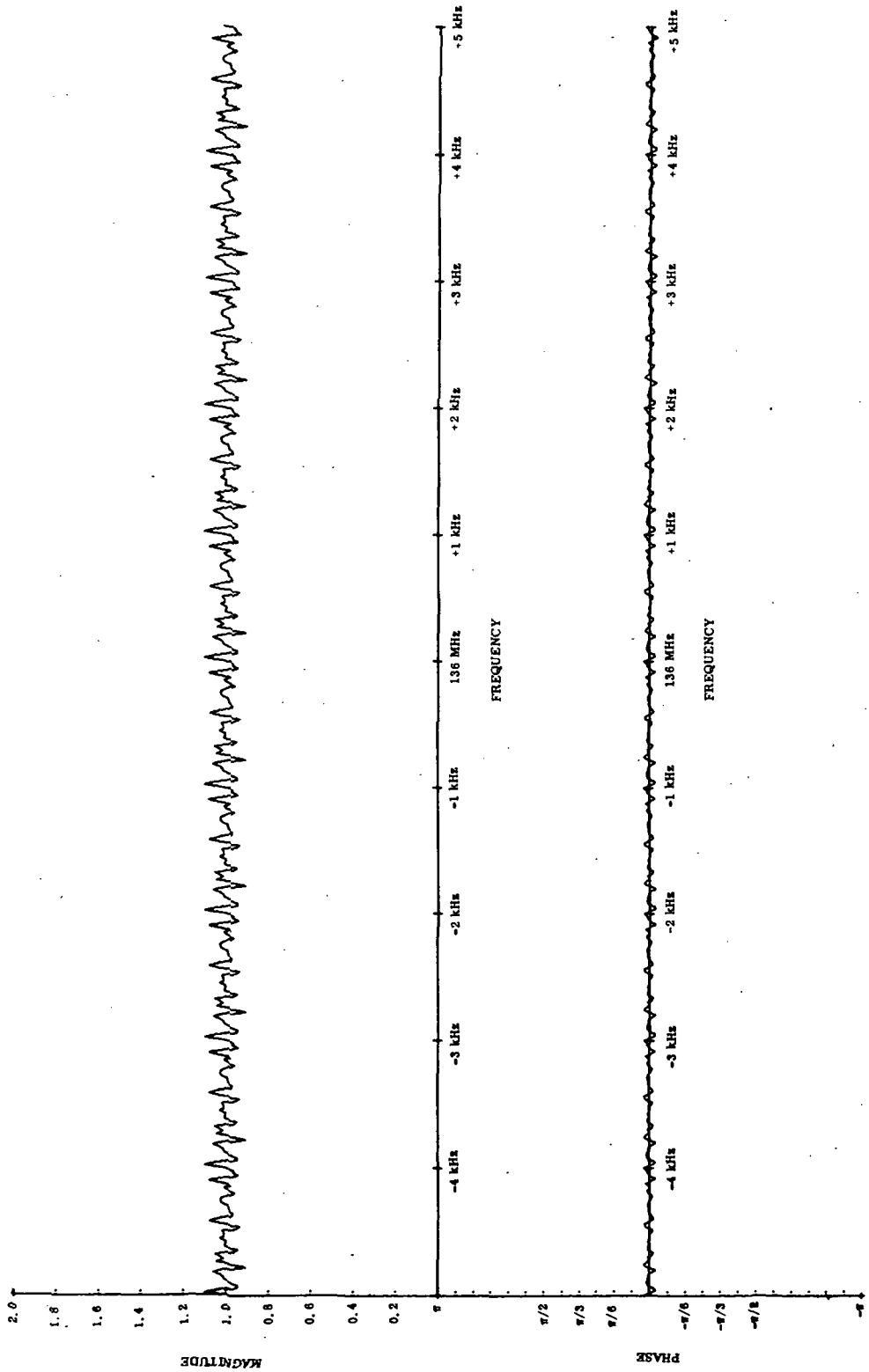

Figure 4-10. Typical Multipath Channel Transfer Function for Weather Satellite/ Synchronous Satellite Relay (Incidence Angle = 70 Degrees)

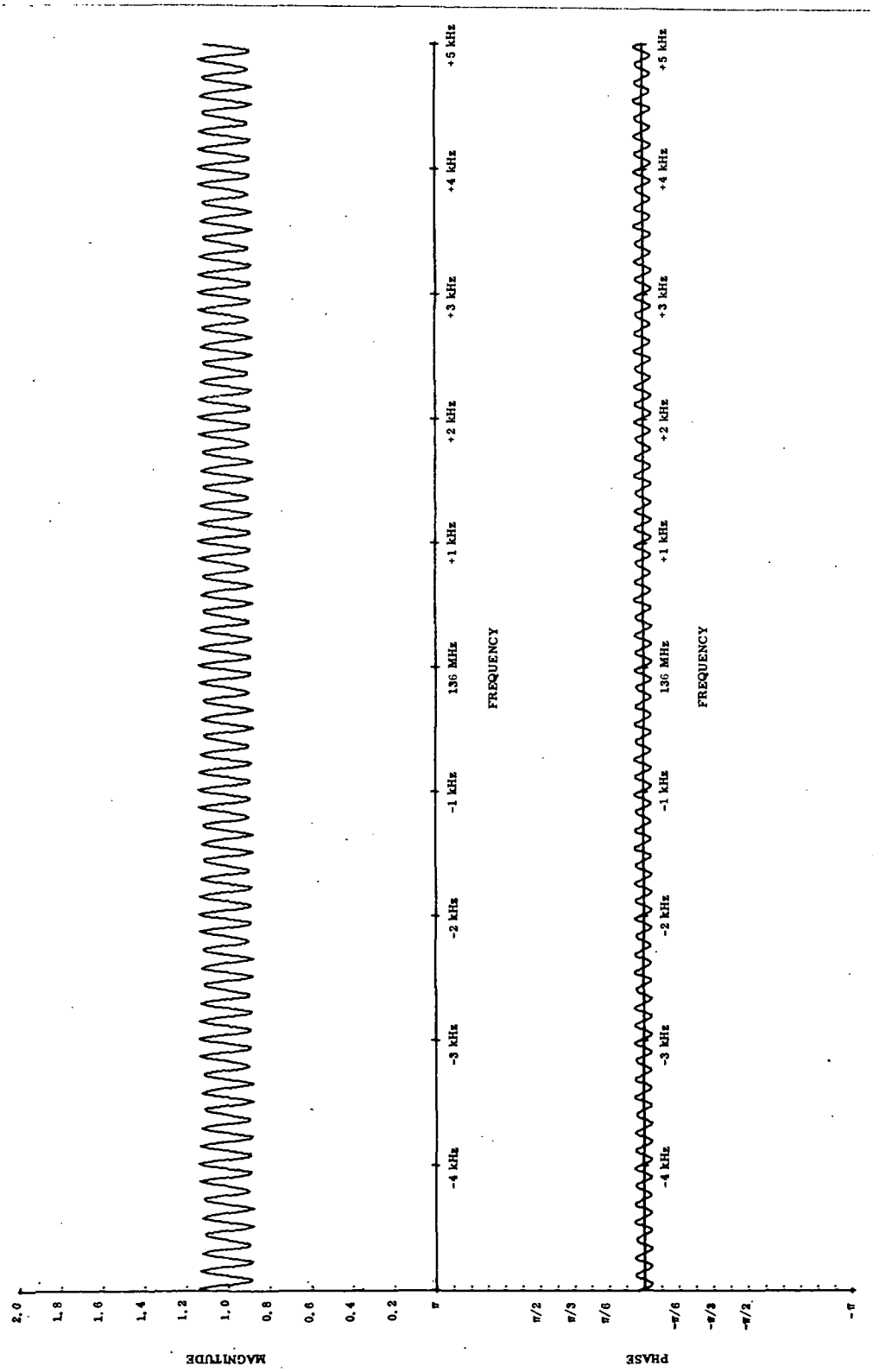

Figure 4-11. Typical Multipath Channel Transfer Function for Weather Satellite/ Synchronous Satellite Relay (Incidence Angle = 80 Degrees)

5. ANTICIPATED ELECTROMAGNETIC INTERFERENCE.

5.1 Noise.

Noise is of interest because it establishes a background level of interference and it is a useful reference base for comparison with other sources of interference. It is convenient to specify noise in a 1 kHz bandwidth because we are interested mainly in digital systems operating at 1 kb/s. The noise power can be readily scaled to other bandwidths of interest. Assuming an 8 dB noise figure for the TDRS receiver, the background noise power is -174 + 30 + 8 = -136 dBm. We can assume that this noise is white and Gaussian in the bandwidth and frequency of interest.

5.2 External Interference.

The anticipated external interference, i.e., interference from sources not a part of the TDRS system, was calculated in an ESL report by applying link calculations to known transmitters.[2] The results were presented in Figures 3-6 and 3-8 of that report for interference between 108 and 170 MHz and geo-stationary satellites located at likely longitudes for the TDRS system. An extract from that report is presented as an example in Figures 5-1 and 5-2 for the 130 to 140 MHz band.

Examination of the ESL results reveals that "typical" interference in the likely frequency band from 136 to 138 MHz is -102 dBm. Peaks 10 dB greater than the "typical" value, and valleys 5 dB less than the "typical" values are not uncommon. However, this noise power appears in a transmission bandwidth that is generally 15 kHz wide

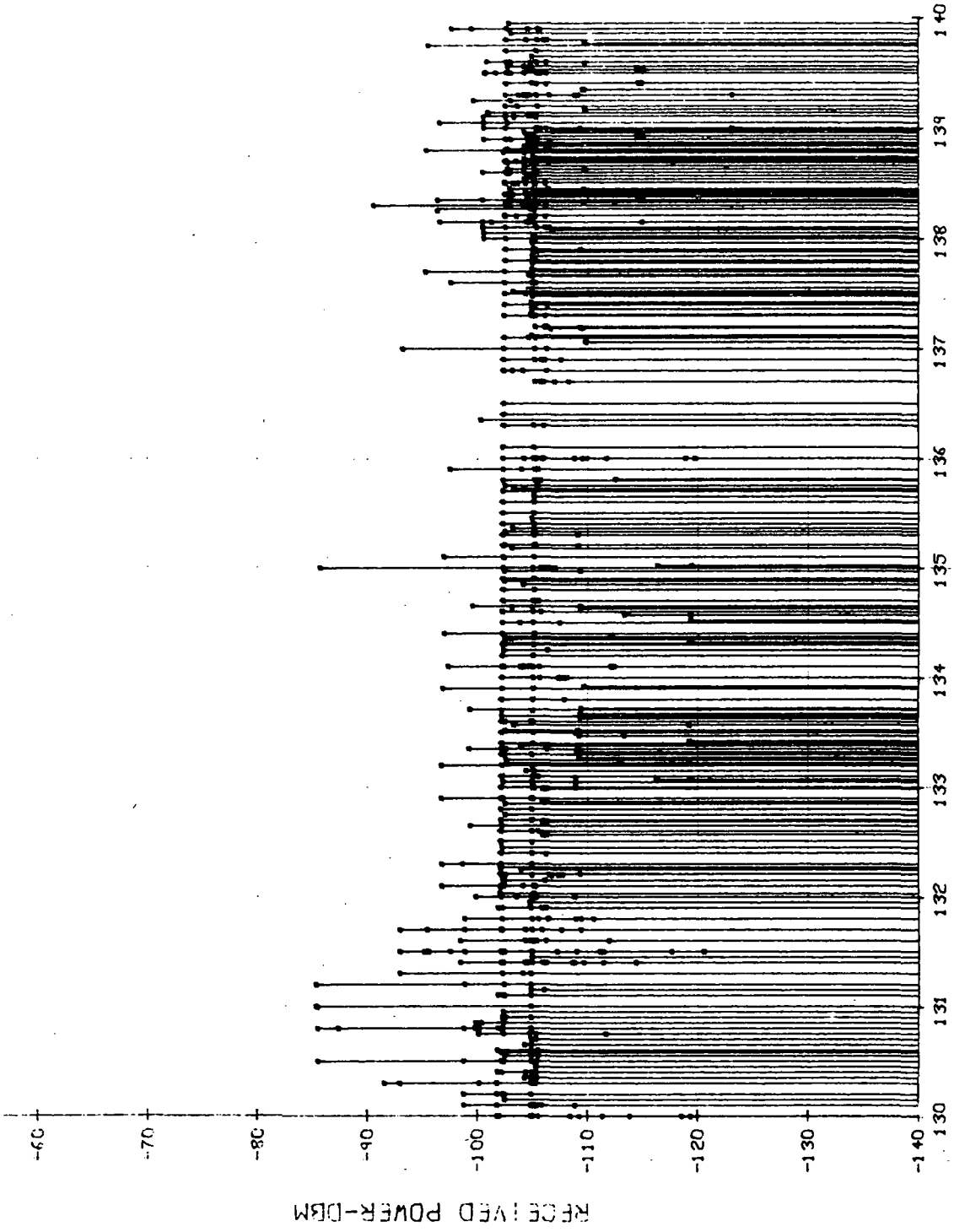

Figure 5-1. Expected External Interference for TDRS at 110°W Longitude

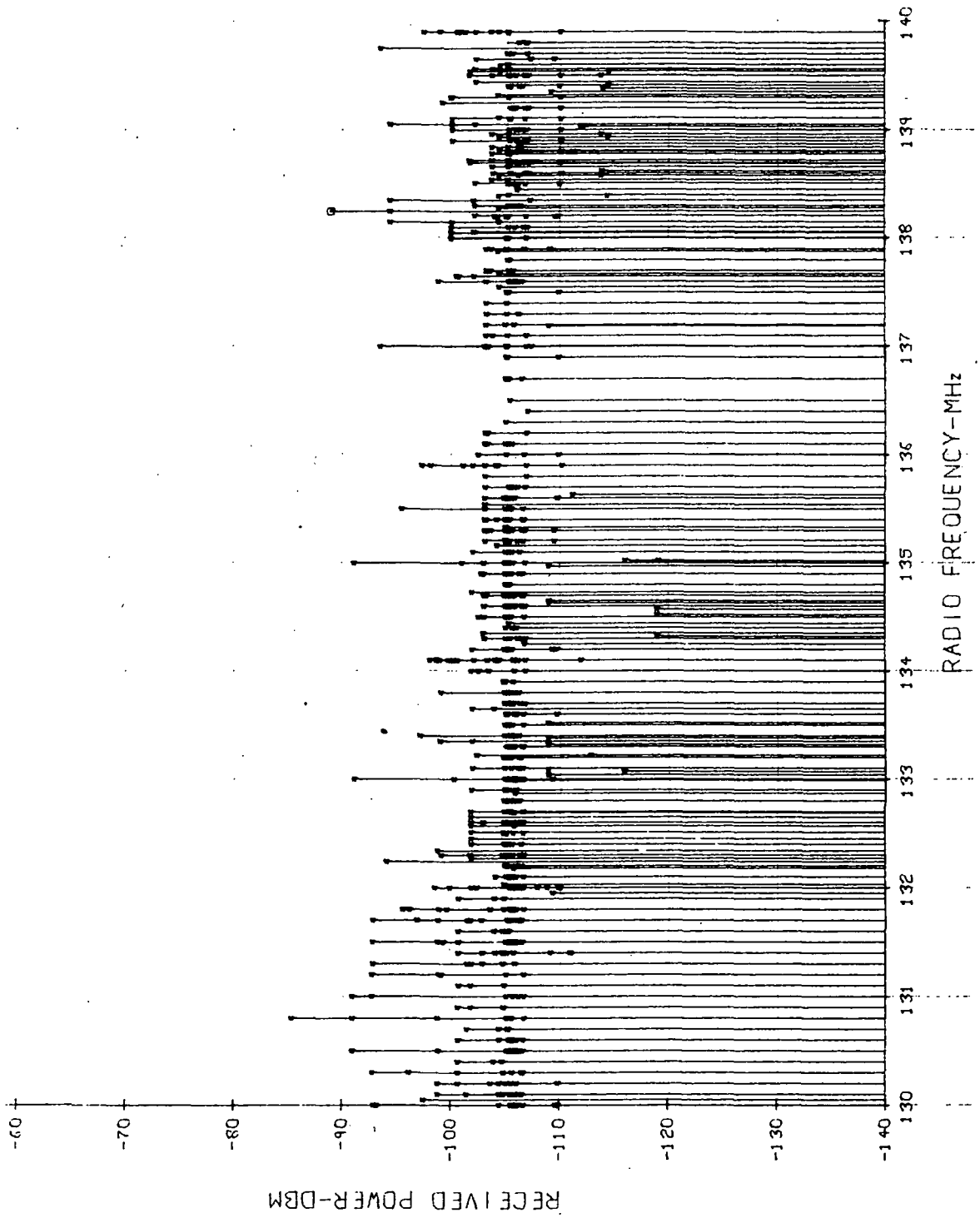

Figure 5-2. Expected External Interference for TDRS at 143°W Longitude

5.2 -- Continued.

compared to the 1 kHz assumed for noise. Therefore, we reduce the interference power by 12 dB in order to properly compare it with noise. Thus, the interference could be 17 to 32 dB greater than the noise. There are also several openings of up to 100 kHz where there is no interference. We can anticipate that there will be 300 to 400 kHz of interference free bandwidth in the 2 MHz from 136 to 138 MHz.

Of cource, the ESL results are uncertain in that they are based on "known" transmitters and assume that these transmitters are operating. Several obvious sources of error are:

a. Existence of transmitters not in the extensive ESL library

b. Low duty cycle of transmitters, particularly those of the push to talk variety

c. Presence in the library of transmitters that are no longer operational

d. Projection of current RFI to future operational systems.

It has been suggested that the actual interference is perhaps 6 dB less than the "typical" value calculated by ESL. This would make the interference peaks 11 to 26 dB greater than the noise, in reasonable agreement with the estimate of Heffernan and Gilchriest[16] that "maximum RFI noise could easily exceed intrinsic thermal noise by as much as 20 to 30 dB." We shall take the value of 20 dB as reasonable for design purposes.

5.3 System Internal Interference.

The different transmitters of the TDRS system can interfere with each other. At one extreme, if the time/frequency assignments are made truly orthogonal (including allowance for time and doppler spread of the signal and multipath), there will be no self interference. The TDRS repeater would also have to be linear to prevent interference from intermodulation products generated in repeater nonlinearities. If the TDRS repeater contained a hard limiter the interference generated by intermodulation products would amount to -8-1/2 dB with respect to the signal.[17] Although intermodulation interference can be reduced by not using the full bandwidth,[18] it is likely that we could not take advantage of this improvement as external interference would appear as additional accesses occupying much of the bandwidth.

At the other extreme, if all transmissions occupy the same time/bandwidth domain, the interference is (N-1) times the desired signal for an N access system. Thus, in a 40 access system, the self interference could be approximately +16 dB with respect to the signal. However, the self interference can be reduced by spectrum spreading techniques. Assuming that a total of 2 MHz is available, and that each access occupies 1 kHz, an improvement equal to the ratio of the bandwidths (33 dB) can be achieved. This would reduce the system self interference to -17 dB which should be satisfactory. Intermodulation interference would not be a problem as the same 33 dB improvement would be realized.

6. PERFORMANCE OF DIGITAL MODULATION.

6.1 Binary PSK.

Our approach to the analysis of different modulation techniques is to begin with a very simple example of a signal that would not necessarily be considered as a likely candidate in the given environment. However, by carrying out some calculations, the good and bad features will be revealed. We can then proceed to examine signals that counteract the problems that are present while preserving the good features.

Consider the use of coherent binary phase shift keying (PSK). The transmitted signal is then

$$s_i(t) = A_i \cos[\omega_i t + \phi_i(t)] \quad .$$

The subscript i denotes the ith signal, assigned to the ith satellite. Each satellite is assigned its own frequency, ω_i, distinct from the remaining. The phase modulation consists of a sequence of discrete values $\pm\pi/2$ with transitions at 0, T, 2T, ... where T is the modulation duration of 1 millisecond for a 1 kb/s signaling rate.

First consider the performance in the presence of specular multipath. Assuming that the satellite repeater is linear, the receiver signal is

$$x_i(t) = A_i \cos[\omega_i t + \phi_i(t)] + B_i \cos[(\omega_i + \omega_d)(t - \tau) + \phi_i(t - \tau)]$$

6.1 -- Continued.

where B_i/A_i is the relative magnitude of the multipath, ω_d is the doppler shift and τ is the relative time delay between signal and multipath. For coherent reception, we multiply the incoming waveform by the local reference

$$r_i(t) = -2 \sin \omega_i t \quad ,$$

and filter out the terms at $2\omega_i$ to obtain

$$y_i(t) = A_i \sin \phi_i(t) + B_i \sin[\omega_d(t-\tau) + \phi_i(t-\tau)] \quad .$$

We now integrate over one pulse

$$z_i(t) = A_i \int_{t=nT}^{(n+1)T} \sin \phi_i(t)\, dt + B_i \int_{t=nT}^{(n+1)T} \sin[\omega_d(t-\tau) + \phi_i(t-\tau)]\, dt \quad .$$

Since $\phi_i(t)$ is either $\pm\pi/2$ with transitions at 0, T, 2T, ... we have

$$z_i(t) = \pm A_i T - B_i \left\{ \pm \int_{t=nT}^{nT+\tau'} \cos[\omega_d(t-\tau)]\, dt \pm \int_{t=nT+\tau'}^{(n+1)T} \cos[\omega_d(t-\tau)]\, dt \right\} \qquad (6\text{-}1)$$

where τ' is the time of possible modulation transition of the multipath signal. The worst case occurs when $\omega_d << 1/T$ and the phase of the modulation on the specular reflection is opposite that of the signal. When this occurs

6.1 -- Continued.

$$z_i(t) = \pm(A_i - B_i)\ T \qquad (6\text{-}2)$$

i.e., the received signal is reduced by B_i. Since the specular multipath can reach -9 dB for the aircraft case at 80 degrees incidence angle (Section 3),* then as a worst case the signal (voltage) is reduced to 0.64 of its normal value. Thus, if noise is present, the signal-to-noise ratio is degraded by 4 dB. Typically, the degradation will be much less than 4 dB because either ω_d will be nonzero, or signal transitions will average out the multipath and at times the phasing of the modulation will enhance the signal. The comparable result for the weather satellite case is -18 dB of specular reflection and a degradation of 1 dB.

The diffuse multipath consists of a large number of random components; thus, it may be regarded as Gaussian noise. Assuming that the spectrum of the diffuse multipath is approximately the same as the signal, the performance is the same as that of PSK in white Gaussian noise. The signal-to-noise ratio is 15 dB for the aircraft case and 22 dB for the weather satellite. Of course, if there is a large doppler shift or spread, we can filter out some of the diffuse multipath and improve the performance. Even without filtering there is 5-1/2 dB and 12-1/2 dB margin, respectively, over the 9-1/2 dB signal-to-noise ratio required for a nominal error rate of 10^{-5}. Combining the specular and diffuse still yields a margin of 4-1/2 dB as the two disturbances are not maximum at the same incidence angles.

*All numerical values of multipath used in this section are taken from Table 3-3 (magnitudes) and Figures 3-9,and 3-10 (dispersion) for the aircraft case and Table 4-2 (magnitudes) and Figures 4-6 thru 4-8 (dispersion) for the weather satellite case.

6.1 -- Continued.

Each PSK signal will occupy approximately 2 kHz of bandwidth between nulls in the spectrum. Allowing another 3 kHz for frequency instability, the entire 40 accesses will require 200 kHz of bandwidth compared to the 300 to 400 kHz of interference free bandwidth that is expected (Section 5). Thus, there is ample room to locate all accesses with no interference if the signals can be commanded to clear channels as interference is observed and the direct doppler is compensated. If another 7-1/2 kHz must be allowed for direct doppler,[14] the system will require more than the available interference-free spectrum.

Since each access is assigned its own frequency, there is no system self interference except for signal side lobes and repeater nonlinearities. With a little pulse shaping (which reduces the signal energy by perhaps 1 dB), filtering, and careful repeater design, we can ignore distortions from self interference.

The performance of PSK in white Gaussian is well known.[19] An energy-to-noise density (signal-to-noise ratio in 1-kHz data bandwidth) of approximately 9-1/2 dB is sufficient for a probability of error of 10^{-5}.

We have summarized the performance of PSK for the aircraft application in Table 6-1. The required signal is 20-1/2 dB greater than the noise; thus, the signal strength must be -115-1/2 dBm. However, no matter how strong the signal is, the margin against diffuse multipath remains barely acceptable (5-1/2 dB). The performance in the weather satellite case is better, 3 dB less received signal is required and the margin against diffuse multipath is a comfortable 12-1/2 dB.

Table 6-1. Performance of PSK

Source of Disturbance	Required Signal Relative to Noise (dB)	Subjective Evaluation
Specular Multipath	4	Poor
Diffuse Multipath	0	Barely acceptable margin
External Interference	0	Excellent
Self Interference	1	Excellent
Noise	9-1/2	Good
Margin	6	--
Total	20-1/2	Good to excellent except multipath

6.2 Spread Systems.

Since the performance of our first system was poorest against multipath we seek a second system that affords protection against multipath. One method of obtaining such protection is to use spread spectrum systems. When the interference (in this case multipath) is not correlated with the signal, an improvement equal to the ratio of the spread bandwidth to the data bandwidth is obtained.* For the moment we are not

*Even greater advantages can be achieved if we can exploit some feature of the interference such as small time spread. However, we assume a worst case for purposes of analysis.

6.2 -- Continued.

concerned with how this spreading is achieved. We assume that the band spread is 10:1 or greater since implementation may not be worth the trouble for lesser amounts.

With a 10 to 1 spread in bandwidth the data "chips" are 0.1 milliseconds long. If the minimum differential time delay exceeds 0.1 millisecond (and it does for all orbits greater than 100 miles) there is no correlation between direct signal and specular multipath and there is a 10 dB improvement in the signal to specular multipath ratio.* Thus, the specular multipath is -19 dB with respect to the signal in the aircraft application, and if it subtracts from the signal (worst case) the reduction in signal amplitude is approximately 1 dB. Of course, spread factors in excess of 10:1 may be necessary in the aircraft application due to the small differential time delay.

The 10 dB improvement in performance against diffuse multipath would yield a margin of 15-1/2 dB in the aircraft application. Thus, the use of 10 dB of spreading would yield satisfactory performance against both specular and diffuse reflections in the aircraft case. Performance is even better when applied to the weather satellite.

The spread signal occupies 20 kHz between nulls in its spectrum. If we add 3 kHz for doppler and other instabilities, a 40 access system occupies 920 kHz if strict orthogonality is preserved. It is highly unlikely that we can find this much bandwidth free of interference as we previously indicated that only 300 to 400 kHz would be available. Since there are numerous sources of external interference, we regard it as Gaussian noise and we must transmit 20 dB more power to overcome it since it is 20 dB greater

*On the average there is no correlation; peaks of correlation will exist and remain to be investigated.

6.2 -- Continued.

than noise. Spreading does not help because additional sources fall in-band, i.e., spreading does not protect against white noise.

As long as the total bandwidth is kept under 2 MHz we can avoid system self interference. The 1 dB for reduced power due to spectral shaping can be removed as the spread protection will obviate the need for spectral shaping. When the spread factor exceeds approximately 23 to 1, system self interference cannot be avoided. However, due to spread protection a judicious choice can be made to keep it reasonably small. Therefore, we assume that no additional signal strength need be allocated to system self interference and that through careful design adequate protection exists.

The noise performance and margin requirements are assumed to be the same as before. The performance of spread spectrum for the aircraft application is summarized in Table 6-2. We see that the price of overcoming multipath by straight spreading is a 16 dB increase in required power for overcoming interference. Performance for the weather satellite application is only 1 dB better due to reduced multipath.

6.3 A Fundamental Choice.

The analysis carried out in Sections 6.1 and 6.2 is a simplified one; yet it illustrates a fundamental design choice. The choice is between interference avoidance or multipath avoidance.

Interference avoidance is achieved with narrow bandwidth systems. As long as the total system bandwidth is less than the available interference free bandwidth, frequency

Table 6-2. Performance of Spread Spectrum

Source of Disturbance	Required Signal Relative to Noise (dB)	Subjective Evaluation
Specular Multipath	1	Good
Diffuse Multipath	0	Excellent
External Interference	20	Very poor
Self Interference	0	Good with care
Noise	9-1/2	Good
Margin	6	--
Total	36-1/2	Good to excellent except external interference

6.3 -- Continued.

assignments can be made which avoid interference and save perhaps 16 dB in effective radiated power. However, narrow bandwidth interference avoiding techniques offer no protection against multipath. Furthermore, implementation will require a central control facility to make frequency reassignments as the interference varies and as the doppler shift varies.

Multipath avoidance is achieved with wide bandwidth systems. As long as the reciprocal of the bandwidth is shorter than the differential time delay, a multipath improvement

6.3 -- Continued.

equal to the ratio of the spread bandwidth to the narrow bandwidth can be achieved. However, the only protection afforded by these systems against interference is the averaging of the interference across all frequencies of the spread bandwidth occupancy.

The analysis carried out in Sections 6.1 and 6.2 suggests that with careful design an interference avoidance system could be built which would require 16 dB or so less effective radiated power than a spread system. However, we are reluctant to recommend it because the performance of such an interference avoiding system depends critically on the estimated parameters. Although we feel that the estimated parameters are the best estimates currently available, we recognize that significant errors might be present which would render a full operational interference avoiding technique unworkable. However, the potential advantage in power is great and one is tempted to at least try such a system in the early phases. A hybrid system which attempts to combine the advantages of both interference avoidance and multipath rejection is described in the following section.

6.4 Possible Hybrid System.

We have seen that it is important to incorporate spread spectrum for protection against diffuse multipath. At the same time the spread spectrum system occupies too much bandwidth for interference protection. Therefore, we investigate a hybrid system where both spreading and narrow banding is used.

6.4 -- Continued.

The signal bandwidth can be reduced by using higher order phase or amplitude shift modulation, i.e., M-ary modulation with M > 2. Unfortunately, the performance in noise deteriorates as M increases. The results are summarized in Table 6-3 for MPSK systems which are more efficient than the amplitude systems.[20] In Table 6-3 we have taken the maximum spread factor to be that multiplier that expands the individual access bandwidth to 10 kHz (system bandwidth 400 kHz) in the absence of allowances for doppler.

A good compromise choice seems to be a quatnary (M = 4) PSK system with a spread factor of 10. The performance results are summarized in Table 6-4.where we see that this hybrid system indeed combines the best features of the systems described in Sections 6.1 and 6.2. It requires 3-1/2 dB less power than the PSK system and 19-1/2 dB less power than spread systems. However, there are some disadvantages as pointed out in the remainder of this section.

The "chips" of the spread spectrum portion of the system are 0.2 milliseconds which is satisfactory for 200-kilometer orbits at 78-degree incidence angle and higher altitudes. At lower altitudes, the differential time delay of the specular component is less than the decorrelation time of the chips; thus full protection against multipath will not be achieved at low altitudes.

The hybrid system occupies 10 kHz per access or 400 kHz for the entire 40 access system. As previously pointed out, it appears that there is a maximum of 400 kHz of interference free bandwidth available. Thus, it appears that there is no bandwidth margin. However, we have specified the bandwidth between nulls of the spectrum and

Table 6-3. Required Signal-to-Noise Ratio for MPSK With $P_e = 10^{-5}$

M	Signal-to-Noise Ratio	Bandwidth Between Nulls (kHz)	Maximum Spread Factor
2	9-1/2	2	5
4	10	1	10
8	13-1/2	1/2	20
16	18-1/2	1/4	40
32	23-1/2	1/8	80

Table 6-4. Performance of Hybrid System

Source of Disturbance	Required Signal Relative to Noise (dB)	Subjective Evaluation
Specular Multipath	1	Good except low altitude
Diffuse Multipath	0	Excellent
External Interference	0	Barely acceptable margin
Self Interference	0	Good with care
Noise	10	Good
Margin	6	--
Total	17	Good to excellent but barely acceptable over certain ranges

6.4 -- Continued.

this can be reduced somewhat providing a small degree of margin. More margin can be provided by cutting the spread factor in half (at the expense of 3 dB of multipath rejection and an increase in required altitude) or by using an 8-phase system (at the expense of 3-1/2 dB more required power). Either of these measures would reduce the required system bandwidth to 200 kHz between nulls which should be adequate.

Doppler shift can be quite severe, amounting to ±4 kHz.[14] If full allowance of 8 kHz is made, the system bandwidth required by the doppler alone would amount to 320 kHz. Thus, it is clear that any interference avoidance system would require a central station not only for making frequency assignments but for adjusting the assignments over the orbital period as the doppler changes.

7. PERFORMANCE OF ANALOG VOICE MODULATION.

7.1 AM.

The AM signal can be written as

$$s_m(t) = [1 + m(t)] \cos \omega_c t \quad .$$

Ignoring the time delay on the modulation $m(t)$, the received AM signal plus specular reflection is

$$x(t) = [1 + m(t)] \cos \omega_c t + R[1 + m(t)] \cos [\omega_c t + \phi(t)]$$

which can be written as

$$x(t) = \{[1 + m(t)] + R \cos \phi [1 + m(t)]\} \cos \omega_c t$$

$$- R \sin \phi [1 + m(t)] \sin \omega_c t \qquad (7\text{-}1)$$

In Equation (7-1), R is the relative amplitude of the specular reflection and $\phi(t)$ is the relative phase angle of the received reflection. Formally, t should be replaced by $t + \lambda$ for the reflected signal; however, the time delays are small relative to what the ear perceives and we ignore it.

If the received signal is coherently detected, by multiplying it in the receiver with a reference generator $2 \cos \omega_c$, we have

7.1 -- Continued.

$$y_c(t) = [1 + m(t)]\,[1 + R\cos\phi] \tag{7-2}$$

Depending on the phase angle ϕ, the received amplitude will increase or decrease by as much as R. In the aircraft application the maximum depth of fade is 4 dB and will occur at approximately a 10 Hz rate while in the weather satellite application* it is 1 dB at approximately 1 kHz. These numerical values are consistent with Section 6 and were taken from Tables 3-4 and 4-2 and from Figures 3-9, 3-10, and 4-6 through 4-8. Fading of 4 dB at 10 Hz would probably be annoying but usable while 1 dB at any rate would be barely noticeable. Of course, the snr would be reduced during the fades.

If an envelope detector were used the received signal is

$$y_e(t) = \left\{[1 + m(t)]^2\,[1 + R^2] + 2\,[1 + m(t)]^2\,R\cos\phi\right\}^{1/2}$$

$$y_e(t) = [1 + m(t)]\left\{[1 + R^2] + 2R\cos\phi\right\}^{1/2} \tag{7-3}$$

When R is small the effects of specular reflection on envelope detected AM are essentially the same as on coherently detected AM.

*Presumably there is no requirement for analog voice from a weather satellite. However, the results are indicative of manned satellites at orbital altitudes.

7.1 -- Continued.

The performance of AM in white Gaussian noise is well known. For nonlinear detectors we have[21]

$$snr_o = m^2 snr_i \tag{7-4}$$

and for coherent detectors[22]

$$snr_o = 2 m^2 snr_i \tag{7-5}$$

where snr_o is the output signal-to-noise ratio, snr_i is the input signal-to-noise ratio and m is the modulation index.

To complete the evaluation of AM we must decide on a reasonable value of modulation index, decide on an acceptable value of output signal-to-noise ratio, and apply the results to the specific cases of aircraft and weather satellites.

The modulation index must be equal to or less than unity to prevent severe distortion and spectrum splatter. At one extreme we can restrict m(t) to ±1 by passing it through a hard limiter. This procedure will maximize the output signal-to-noise ratio in accordance with Equations (7-4) and (7-5). The clipped voice will sound distorted but will still be usable. At the other extreme, if no nonlinear processing is used, the quality of the voice will be better but a much smaller modulation index (and consequently output snr) must be used to prevent overmodulation. Experimental curves of Bell

7.1 -- Continued.

System subscribers suggest that the backoff would have to be 12 dB to prevent overmodulation more than 1 percent of the time.[23] Presumably, the more formal training of aircraft pilots and astronauts would reduce the variance. Alternatively, nonlinearities other than hard limiters (e.g., companders) could be used to reduce the variance. Consequently, it appears that the modulation index can be anywhere between unity and -12 dB. We shall arbitrarily use -6 dB in our calculations, i.e., the output snr will be reduced by 6 dB to prevent overmodulation.

Extensive intelligibility testing in white Gaussian noise has shown that when the snr is 10 dB, word intelligibility is approximately 97 percent.[24] These tests were conducted in a 6 kHz bandwidth which is wider than normal and tends to give optimistic results. However, the tests were performed with phonetically balanced word lists which tend to lower scores by eliminating word context. We shall accept 10 dB as a reasonable signal-to-noise ratio.

Combining the results of the preceding paragraphs we see that the input snr should be 16 dB for nonlinear detectors and 13 dB for coherent detectors in order to have an adequate voice output. However, we recognize that the results are quite subjective.

We now apply the results to the aircraft case. The diffuse multipath, which can be modeled as white Gaussian noise, can be as strong as -15 dB. This would be 1 dB more than acceptable for nonlinear detectors and would provide only 2 dB margin for coherent detectors. The presence of specular multipath would lower the performance by approximately 1 dB as the worst case specular does not occur simultaneously with worst case diffuse. Since AM has a relatively narrow RF bandwidth we can avoid

7.1 -- Continued.

external interference and internal self interference if there are not too many simultaneous accesses (the 40 accesses used in Section 6 applied only to data). The performance in noise requires an input snr of 13 to 16 dB plus margin where the noise is taken in the input bandwidth which is twice the modulation bandwidth. The performance for the weather satellite application is better since the maximum diffuse multipath is -22 dB and occurs when the specular multipath is negligible.

7.2 FM.

The analysis of FM disturbed by a specular reflection is much more complicated than the corresponding analysis of AM. In the FM case we may ignore the amplitude variations as they will be removed in the limiter-discriminator. However, phase variations are produced which will be detected. These phase variations will not have the same form as the desired phase modulation and will consequently appear as noise rather than subtraction of signal. Furthermore, the phase variations will depend critically on the phasing between desired signal and reflection.

A thorough analysis of the distortion of FM produced by a specular reflection has been carried out by assuming that the modulation is a band of white noise and the effect of the distrotion is also noise-like.[25] The results for the worst case phase angle are shown in Figure 7-1. We need only apply this figure to our two cases.

In the aircraft case, the maximum differential time delay is 67 microseconds. Assuming that the maximum modulating frequency of voice is 4 kHz, the parameter

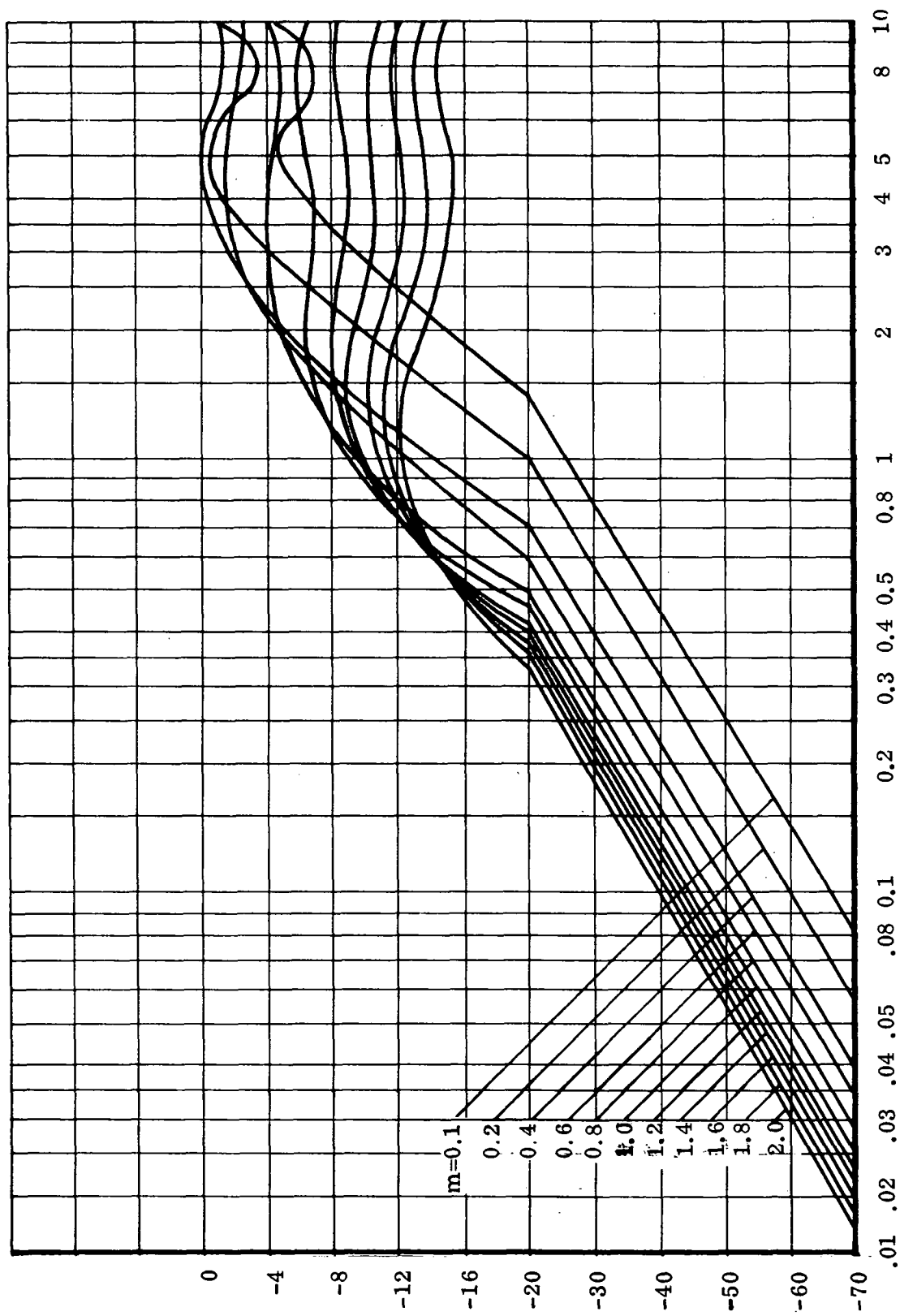

Figure 7-1. Output Distortion of FM With Specular Reflection at Worst Phasing; Source: Medhurst[25]

7.2 -- Continued.

$\omega\tau$ takes on a value of 1.68. The distortion also depends on the modulation index. We shall take the minimum modulation index as 0.5 which corresponds to the 6 dB backoff used in the AM case. This value will yield noise performance comparable to AM. From Figure 7-1, the signal to distortion ratio is approximately 10 dB minus the magnitude of the reflected signal in decibels. Thus the output signal-to-distortion ratio is approximately 19 dB. If we increase the modulation index, the distortion will first increase (by 3-4 dB) and then begin to decrease. However, our results are pessimistic in that we have assumed the maximum differential time delay whereas the maximum specular reflection occurs at high incidence angles where the time delay and distortion is much less.

For the weather satellite application, the specular reflection is at most -18 dB. Applying Figure 7-1 for long time delays we see that the signal-to-distortion ratio is at least 18 dB and increases with modulation index.

The performance of FM in white Gaussian noise is well known and is given by[21]

$$snr_o = 3\, m^2\, snr_i$$

assuming as we do here that the input snr is above threshold. Thus, if we use the same modulation index as AM (0.5), then FM will perform 4.8 dB better than nonlinear detection of AM and 1.8 dB better than coherent detection. If we raise the modulation index to unity, we gain an additional 6 dB which is needed for margin. The penalty for increasing the modulation index is an increase in bandwidth to approximately twice

7.2 -- Continued.

that of AM, making it more susceptible to interference and raising the distortion caused by specular reflections. If the modulation index is increased further to a value of two, the distortion caused by specular reflections is no worse than -21 dB and the performance against diffuse multipath and noise improves by another 6 dB. However, the bandwidth is approximately three times that of AM making the wideband FM more vulnerable to interference. A further increase in modulation index is probably inadvisable due to threshold effects. We could also linearly sweep the FM as a multipath rejection technique but the bandwidth for snr exchange is less favorable.

To summarize, narrow-band FM (m = 0.5) is slightly better than AM but is still marginal. Wideband FM with a modulation index of perhaps two would improve performance to significantly above the marginal region provided that sufficient system bandwidth is available.

8. REFERENCES.

1. P. F. Barritt and E. J. Habib, "Tracking and Data Relay Satellite System: An Overview," Presented at AIAA 7th Annual Metting, Houston, Texas, October 1970.

2. J. A. Jenny and S. J. Weiss, The Effects of Multipath and RFI on the Tracking and Data Relay Satellite System, ESL Incorporated, TM 215, 18 March 1971.

3. Petr Beckmann and Andre Spizzichino, The Scattering of Electromagnetic Waves From Rough Surfaces, MacMillan Co., New York, 1963.

4. M. Slack, "The Probability Distribution of Sinusoidal Oscilations Combined in Random Phase," J. IEE Part III, Vol. 93, March 1946; pp 76-86.

5. M. Schwartz, W. R. Bennett, and S. Stein, Communication Systems and Techniques, McGraw-Hill Book Co., New York, 1966, p 349.

6. S. O. Rice, "Statistical Properties of a Sine Wave Plus Random Noise," Bell System Technical Journal, Vol. 27, January 1948, pp 109-157.

7. K. A. Norton, L. E. Vogler, W. V. Mansfield, and P. J. Short, "The Probability Distribution of the Amplitude of a Constant Vector Plus a Rayleigh-Distributed Vector," IEEE Proceedings, October 1955, pp 1354-1361.

8. T. Kailath, "Channel Characterization: Time Variant Dispersive Channels," in Lectures on Communication System Theory, ed. by E. J. Baghdady, McGraw-Hill, New York, 1961.

9. R. F. Daly, T. Kailath, and P. D. Shaft, "Limitations of Radio Propagation Media" WESCON 67, paper 9/2, San Francisco, Calif. August 1967.

10. L. J. Page and P. C. Chestnut, A Rough Earth Scattering Model for Multipath Prediction, ESL Incorporated, Report ESL-PR53, June 1970.

11. G. T. Bergemann and H. L. Kucera, "Signal Characteristics of a Very High-Frequency Satellite-to-Aircraft Communications Link," IEEE Transactions on Communication Technology, Vol. COM-17, No. 6, December 1969, pp 677-685.

8. - -- Continued.

12. F. E. Bond and H. F. Meyer, "Fading and Multipath Considerations in Aircraft Communications Systems," Communication Satellite Systems Technology, R. B. Marsten, ed., Academic Press, New York, 1966, p 196.

13. K. L. Jordan, "Measurement of Multipath Effects in a Satellite-Aircraft UHF Link," IEEE Proceedings (Letters), June 1967, pp 1117 and 1118.

14. Tom Golden, Range and Velocity Components of TDRS Multipath Signals, Goddard Space Flight Center Report X-520-69-38, February 1969.

15. S. H. Durrani and H. Staras, "Multipath Problems in Communications Between Low-Altitude Spacecraft and Stationary Satellites," RCA Review, March 1968, pp 77-105.

16. P. J. Heffernan and C. E. Gilchriest, "A Multiple-Access Satellite Relay System for Low Data Rate Users" WESCON 69, San Francisco, Calif., August 1969.

17. C. R. Cahn, "Crosstalk Due to Finite Limiting of Frequency-Multiplexed Signals." Proc. IRE, Vol. 48, pp 53-59, January 1960.

18. P. D. Shaft, "Intermodulation Interference in Frequency-Division Multiple Access" Third International Conference on Communications; Minneapolis, Minn., June 1967.

19. J. M. Wozencraft and I. M. Jacobs, Principles of Communication Engineering, Wiley, New York 1967.

20. C. R. Cahn, "Performance of Digital Phase Modulation Communication Systems Systems," IRE Trans. on Comm. Sys. Vol. CS-7, pp. 3-6, May 1959.

21. M. Schwartz, Information Transmission, Modulation, and Noise, McGraw-Hill, New York 1959, Chapter 6.

22. P. F. Panter, Modulation, Noise, and Spectral Analysis, McGraw-Hill, New York, 1965, Chapter 6.

8. -- Continued.

23. K. L. McAdoe, "Speech Volumes on Bell System Message Circuits," Trans. AIEE, Part I, No. 59, pp. 8-13, March 1962.

24. R. J. Christman, G. E. Renaud, and A. Rubin, "The Effect of Speech and Noise Levels on the Masking of Speech by Pure Tones and Random Noise" Rome Air Dev. Center Report RADC-TN-60-97, July 1960. (AD 241096)

25. R. G. Medhurst, "Echo-Distortion in Frequency Modulation," Electronic and Radio Engineer, Vol. 36, pp. 253-259, July 1959.